Transmission Probability and Power Optimization for Covert Communications in UAV-Aided THz Wireless Networks

Xinzhe Pi, Bin Yang, Yulong Shen, Xiaohong Jiang, Tarik Taleb

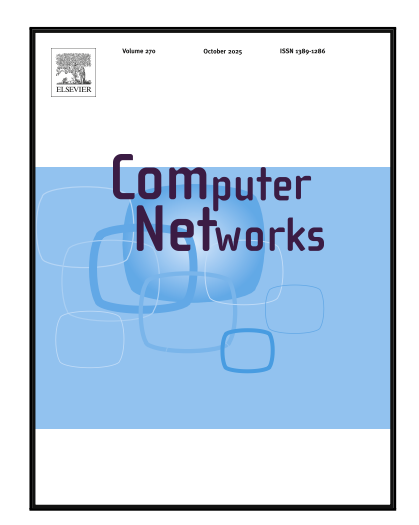
PII: \$1389-1286(25)00754-6

DOI: https://doi.org/10.1016/j.comnet.2025.111788

Reference: COMPNW 111788

To appear in: Computer Networks

Received date: 6 March 2025 Revised date: 8 September 2025 Accepted date: 14 October 2025



Please cite this article as: Xinzhe Pi, Bin Yang, Yulong Shen, Xiaohong Jiang, Tarik Taleb, Transmission Probability and Power Optimization for Covert Communications in UAV-Aided THz Wireless Networks, *Computer Networks* (2025), doi: https://doi.org/10.1016/j.comnet.2025.111788

This is a PDF of an article that has undergone enhancements after acceptance, such as the addition of a cover page and metadata, and formatting for readability. This version will undergo additional copyediting, typesetting and review before it is published in its final form. As such, this version is no longer the Accepted Manuscript, but it is not yet the definitive Version of Record; we are providing this early version to give early visibility of the article. Please note that Elsevier's sharing policy for the Published Journal Article applies to this version, see: <a href="https://www.elsevier.com/about/policies-and-standards/sharing#4-published-journal-article">https://www.elsevier.com/about/policies-and-standards/sharing#4-published-journal-article</a>. Please also note that, during the production process, errors may be discovered which could affect the content, and all legal disclaimers that apply to the journal pertain.

© 2025 Elsevier B.V. All rights are reserved, including those for text and data mining, Al training, and similar technologies.

# Transmission Probability and Power Optimization for Covert Communications in UAV-Aided THz Wireless Networks

Xinzhe Pi<sup>a,\*</sup>, Bin Yang<sup>a</sup>, Yulong Shen<sup>b</sup>, Xiaohong Jiang<sup>c</sup> and Tarik Taleb<sup>d</sup>

#### ARTICLE INFO

# Keywords: Covert communication THz wireless network UAV IoT throughput optimization

#### ABSTRACT

Terahertz (THz) wireless networks assisted by unmanned aerial vehicles (UAVs) can enable highspeed, line-of-sight (LoS) wireless communications using directional antennas in the THz bands, specifically for 6G network applications. However, such networks also suffer from the challenge of sensitive information leakage once an attacker resides in the signal beam. We investigate joint transmission probability and power optimization for wireless covert communications in a UAVaided THz wireless network (UTWN) composed of a transmitter, a UAV relay, a receiver, and two UAV wardens, where these two wardens attempt to detect the presence of wireless transmissions across two respective hops. Specifically, we first derive the minimum detection error probability (DEP) associated with information transmission probabilities and power at the transmitter and UAV relay. We then model the average covert throughput (ACT) and formulate the maximum ACT as an optimization problem, considering constraints such as covertness requirement, information transmission probability, and power. Additionally, we introduce a heuristic algorithm aimed at solving the optimization problem through the joint optimization of information transmission probabilities and power in two hops. Finally, we present simulation and numerical results to validate our theoretical analysis and also to illustrate the impacts of network parameters on the maximum ACT. Assuming that wardens know or correctly guess the prior probabilities of covert transmissions over two hops in their hypothesis testing, we find that prior probabilities are not always equal to 0.5 when achieving maximum ACT in the UTWN, which indicates that covert communications with general prior probabilities and such wardens need more consideration and discussion.

#### 1. Introduction

Terahertz (THz) band from 0.1 to 10 THz is of paramount significance for enabling a massive number of connected Internet of Things (IoT) devices in 6G and beyond wireless networks [1][2]. In particular, the abundant spectrum resources over the THz band can achieve ultra-high data rate and overcome current spectrum scarcity limitation for wireless communications. However, THz communications suffer from high propagation loss, molecular absorption and lineof-sight (LoS) blockage, which severely limits the communication range. Due to flexible deployment, high mobility and less blockage effect of unmanned aerial vehicles (UAVs), UAV-aided THz wireless networks (UTWNs) can significantly expand the THz communication range for meeting the requirements of various 6G network applications [3][4]. In addition, highly directional antennas are usually utilized to enhance the THz communication performance, while narrow beams are also helpful in avoiding eavesdropping and improving communication security of UTWNs.

However, such networks still face security challenges once eavesdroppers reside in the antenna beam. Recently, covert communications have emerged as a promising technology to provide strong security and privacy protection,

≥ pixinzhe@gmail.com (X. Pi); yangbinchi@gmail.com (B. Yang);
ylshen@mail.xidian.edu.cn (Y. Shen); jiang@fun.ac.jp (X. Jiang);
tarik.taleb@rub.de (T. Taleb)
ORCID(s):

through utilizing random characteristics of channels (e.g., noise) to prevent wardens from detecting the existence of wireless communications [5]. Therefore, it is essential to explore covert communications in UTWNs for supporting security-sensitive IoT applications like autonomous driving [6].

Notice that only a small amount of research has explored the emerging THz covert communications by now. A further understanding of THz covert communications is critical to ensuring the security of confidential information transmissions in future 6G wireless networks. In particular, the covert communication studies over THz frequency differ from those over conventional radio frequency (RF) in wireless networks. Since highly directional antennas over THz frequency result in very poor signals outside the THz signal beam, a warden outside the beam cannot effectively detect THz signals but can do so well on RF signals. Thus, multiple wardens are required to detect the multi-hop transmissions, and each warden can only detect THz signals in one hop. Additionally, the transmission probabilities of source and relay in wireless networks can also significantly affect prior probabilities of their covert transmissions and further influence network performance, such as each warden's detection performance and covert throughput. Here, the prior probabilities represent the probabilities of transmission occurring and no occurring associated with the transmission probabilities and outage probabilities. The existing works mainly consider that the warden is completely unaware of

<sup>&</sup>lt;sup>a</sup>School of Computer and Information Engineering, Chuzhou University, Chuzhou, 239000, China

<sup>&</sup>lt;sup>b</sup>School of Computer Science and Technology, Xidian University, 710071, Xi'an, China

<sup>&</sup>lt;sup>c</sup>School of Systems Information Science, Future University Hakodate, Hakodate, 041-8655, Japan

<sup>&</sup>lt;sup>d</sup> Faculty of Electrical Engineering and Information Technology, Ruhr University Bochum, Bochum, 44801, Germany

Transmission Probability and Power Optimization for Covert Communications in UAV-Aided THz Wireless Networks

transmission occurring. Thus, a common assumption is that covert transmission occurs with a probability of 50%, i.e., equal prior probabilities. An interesting issue is to explore how transmission probability affects covert performance in wireless networks if wardens are aware of prior probabilities.

Based on these above observations, this paper investigates THz covert communications in a UTWN with two wardens, where the transmission probabilities at the source and relay can be flexibly controlled such that they can cover the prior probabilities of 50% as their special case. We explore ACT maximization by jointly optimizing covert transmission probabilities and power in two hops. The main contribution of this paper is summarized as follows.

- We explore THz covert communications in a UTWN consisting of a transmitter (Alice), a UAV relay, a receiver (Bob), and two UAV wardens (Willie and Sam), where Willie and Sam detect the transmissions of Alice and relay, respectively. Regarding the UTWN, we derive the detection error probabilities (DEPs) of Willie and Sam, the corresponding minimum DEPs and optimal thresholds. Then, the overall DEP of wardens is defined as the smallest one among their minimum DEPs.
- We model the average covert throughput (ACT) and formulate maximum ACT as an optimization problem with the constraints of covert requirement, transmission probabilities of Alice and relay, and their transmission power. To solve this optimization problem, we further propose a genetic algorithm to maximize ACT by jointly optimizing transmission probabilities and power in two hops.
- Extensive simulation and numerical results are presented to validate our theoretical analysis and also to show the impacts of key parameters on covert performance in the UTWN.

The rest of this paper is organized as follows. Section II introduces the related works. Section III introduces the system model in our work. Section IV explores the covert performance of the UTWN. The formulation of the optimization problem is shown in Section V. We provide numerical results in Section VI. Finally, this paper is concluded in Section VII. The main notations of this paper are summarized in Table 1, where t and r denote a transmitter and a receiver, respectively.

#### 2. Related Work

The existing research works on covert communications mainly focus on wireless networks with and without the help of relay. For covert communications without relay, the pattern between signal power and covert performance is usually analyzed while satisfying the covertness constraint since stronger signals are easier for wardens to detect. To further improve covert performance, cooperative jamming technology is employed to hide the covert signals, in which

Table 1
Main Notations

Notation		Definition		
$h_{t}$	r	Channel coefficient between $t$ and $r$		
$h_t$ $\sigma_t^2$	2 r	Variance of $h_{tr}$		
$g_t$		Channel gain between $t$ and $r$		
$d_t$	r	Distance between $t$ and $r$		
$\gamma_t$	r	SINR between $t$ and $r$		
$\gamma_{\rm t}$		SINR threshold		
$\mathbb{P}_o$	,tr	Outage probability of $t$ 's transmission to $r$		
$T_t$	r	Channel throughput between $t$ and $r$		
$\eta_{_A}$ ,	$\eta_R$	Transmission probability of Alice and relay		
$\pi_{\scriptscriptstyle{A,0}}$ ,	$\pi_{{\scriptscriptstyle A},1}$	Prior probabilities of Alice's transmission		
$\pi_{R,0}$ ,	$\pi_{R,1}$	Prior probabilities of relay's transmission		
$ au_{_W}$ ,	$ au_{S}$	Thresholds of Willie's and Sam's detection		
$P_A$ ,	$P_R$	Transmission power of Alice and relay		
$P_{\rm m}$	ax	Maximum transmit power of Alice and relay		
$P_W$ ,	$P_S$	Power of received signals at Willie and Sam		
$I_R$ ,		Interference power of relay and Bob		
$N_A$ , $N$	$_{R}$ , $N_{B}$	Noise power at Alice, relay and Bob		
$N_W$ ,	$N_S$	Noise power at Willie and Sam		
$\mathbb{P}_{FA,W}$ ,	$\mathbb{P}_{MD,W}$	FA and MD probabilities of Willie		
$\mathbb{P}_{FA,S}$ ,		FA and MD probabilities of Sam		
$\mathbb{P}_{e,W}$ ,	$\mathbb{P}_{e,S}$	DEPs of Willie and Sam		
P		Overall DEP of wardens		
$\bar{I}$	7	Average throughput		
$\overline{T}_{\rm cn}$	nax	Maximum average covert throughput		
$f_X$	(·)	Probability density function of $X$		
$F_X$	(·)	Cumulative density function of $X$		

friendly jammer injects artificial noise to confuse the detector's decision on wireless transmissions [7][8][9][10][11]. Besides, covert communications are studied under random transmit power [12], rate control [13], full-duplex communication mode [14][15] and different channel conditions in wireless networks, such as partial channel state information (CSI) [16].

As for covert communications with relay, cooperative jamming [17], full-duplex communication mode and transmission power control [18][19] are utilized to improve the performance of covert transmissions in wireless networks. The scenario of finite blocklength communication is also explored in relay-assisted covert communication [20]. The work in [21] proves that covertness can be achieved under different relay-forwarding modes in terms of amplify-and-forward (AF) and decode-and-forward (DF). Relay selection schemes are further proposed to improve covert performance [22][23]. Some recent works adopt a promising intelligent reflective surface (IRS) serving as a relay to assist covert communications [24][25]. In [26], the wireless communication with both covertness and security requirements is also discussed in a UAV-assisted relay system.

A few initial works have been devoted to exploring covert communications in THz wireless networks [27], [28] and [29]. The study presented in [27] examines the throughput of covert communication within an IoT network that incorporates both low-frequency Additive White Gaussian

Transmission Probability and Power Optimization for Covert Communications in UAV-Aided THz Wireless Networks

Noise (AWGN) and THz channels. The authors observe that covert communication in IoT networks with the THz band presents greater challenges. This is due to the fact that adversaries can readily position a receiver within the narrow beam connecting Alice and Bob, thereby facilitating the detection or obstruction of their LoS communications. In [28], a novel distance-adaptive absorption peak modulation technique is introduced for THz covert communications, exploring the frequency-dependent molecular absorption. Numerical findings demonstrate that compared to random spectrum selection methods, this proposed technique effectively reduces the eavesdropping distance of a warden. Mamaghani et al. investigate covert communication for securely transmitting confidential data from an access point (AP) to multiple ground user equipments (UEs) within an IoT network, utilizing a UAV-mounted IRS operating across THz frequency bands, as detailed in reference [29]. They propose and solve the energy efficiency optimization problem with the constraints of transmission power, interference power, IRS beamforming, UAV trajectory, and UAV speed using the block successive convex approximation (BSCA) approach. In [30], we model the average covert throughput in a THz wireless network with multiple wardens, where the prior probabilities of Alice's and relay's transmissions are assumed to be equal and the throughput maximization is not explored. Recently, authors in [31] investigate a multiuser covert THz communication system with a warden and a legitimate receiver under the constraint of outdated CSI and data exception.

To clearly illustrate the novel contributions of this paper, we explicitly clarify the differences between our work and existing studies [29], [30], and [32]. In [32], the authors investigate the covert performance of single-hop covert communications against multiple randomly distributed wardens within a two-dimensional model. In [29], the authors consider a scenario where the channels between a terrestrial AP and multiple ground users are obstructed. They employ a UAV-mounted IRS to facilitate communication between the AP and a selected UE, regarding all other UEs as potential wardens. However, their analysis and discussion of covertness are limited to the reflected signals, i.e., the signals in the second hop, while neglecting the covertness of signals in the first hop. In [30], we analyze and explore twohop covert communications in a UAV-assisted THz network, requiring the signals in both the first and second hops to be covert. Nevertheless, we do not investigate the impact of the transmission probabilities of Alice and the relay on covert performance in [30], nor do we formulate optimization problems, design algorithms, or solve the optimization problem of covert performance. In contrast to the aforementioned works, this study investigates the performance and optimization of covert communications in a UAV-assisted THz network under the requirement that signals in both hops are covert. Our objective is to identify the optimal transmission power and optimal transmission probabilities for Alice and the relay to maximize the average covert throughput.

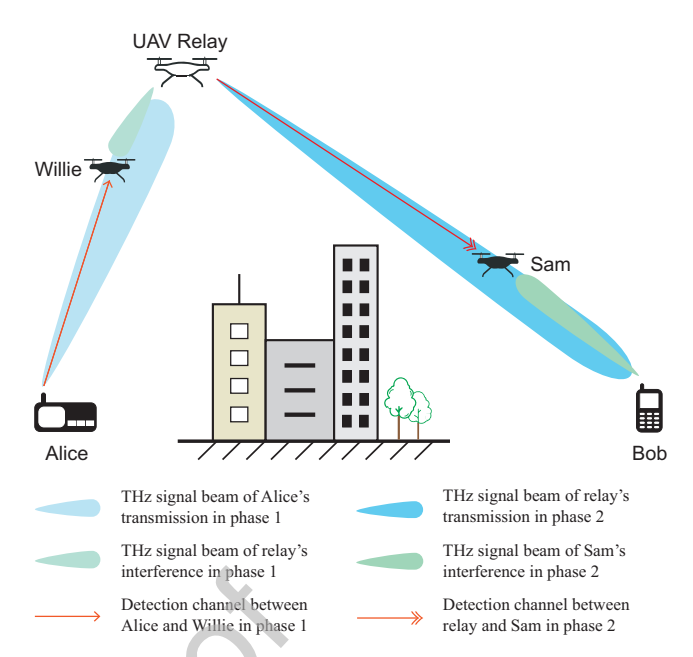


Figure 1: The covert UAV-aided THz wireless network.

#### 3. System Model

#### 3.1. Network Model

As depicted in Fig.1, we consider a covert UTWN comprising a transmitter (Alice), a receiver (Bob), two UAV wardens (Willie and Sam) and a UAV relay. The UAV relay provides LoS links and extends the transmission distance for THz transmissions. Alice endeavors to covertly send confidential messages to Bob through the UAV relay's forwarding, while Willie and Sam detect the presence of the wireless transmissions from Alice and the UAV relay, respectively. The relay operates in decode-and-forward (DF) mode and forwards Alice's messages to Bob.

We assume that wardens, Willie and Sam, are located in the main lobe area between the transmitter and the receiver in two hops, respectively, and regard this scenario as the worstcase scenario for covert THz communication in this work. This is the worst-case scenario because wardens in the main lobe area close to the transmitter will achieve good detection performance since the signal strength at wardens is high. It is very challenging to achieve covertness of transmissions against such wardens. To help cover the transmissions over two hops, we apply the cooperative interference technology in the UTWN. The relay and Bob emit interference signals of power  $I_R$  and  $I_B$ , respectively. In the UTWN, we decide the values of  $I_R$  and  $I_B$  considering the power consumption, battery capacity and expected runtime at the UAV relay and Bob. Additionally, the relay and Bob apply the selfinterference cancellation (SIC) technique to eliminate the self-interference from interference signals. The process of covert communication is composed of the following two phases.

**Phase 1**: In the first phase, Alice transmits confidential information to the UAV relay with a probability  $\eta_A$  and transmission power  $P_A$ . At the same time, the relay emits

Transmission Probability and Power Optimization for Covert Communications in UAV-Aided THz Wireless Networks

Case No.	Case Description	Scenario		Probability of this case	
1	Alice does not transmit messages.	Alice	F@S Relay	کی شف Bob	$1-\eta_A$
2	Alice transmits messages; Relay fails to decode and thereby cannot forward.	Alice	Relay X	S) Bob	$\eta_A \mathbb{P}_{o,AR}$
3	Alice transmits messages; Relay decodes successfully; Ray does not forward.	Alice		S) Bob	$\eta_A (1 - \mathbb{P}_{o,AR})(1 - \eta_R)$
4	Alice transmits messages; Relay forwards messages; Bob fails to decode.	Alice		→ ∰ Bob <mark>X</mark>	$\eta_A ig(1 - \mathbb{P}_{o,AR}ig) \eta_R \mathbb{P}_{o,RB}$
5	Alice transmits messages; Relay forwards messages; Bob decodes successfully.	Alice	Relay √	→ Š) Bob√	$\eta_A ig(1 - \mathbb{P}_{o,AR}ig) \eta_R ig(1 - \mathbb{P}_{o,RB}ig)$

Figure 2: Different cases of two-hop communications.

interference signals with transmission power  $I_R$  to hinder Willie's detection.

**Phase 2:** In the second phase, the relay forwards information to Bob with a probability  $\eta_R$  and transmission power  $P_R$  if the received signals are successfully decoded. Concurrently, Bob emits interference signals to impede Sam's detection with transmission power  $I_R$ .

Transmission probability is the probability of transmitting signals for Alice and the relay when there are messages to be sent, which is a conditional probability. Therefore, transmission probability is only meaningful when there are messages to be sent. In this work, Alice, as the initiator of the two-hop transmission, must have messages to send. Alice decides whether to send messages to the DF relay with probability  $\eta_A$ . If Alice sends messages, relay would receive signals from Alice and tries to decode the signals. If the signal-to-interference-and-noise ratio (SINR) of relay's received signals is smaller than a predefined threshold  $\gamma_{th}$ , relay cannot obtain Alice's messages from the signals and thereby can not forward messages. Only when relay successfully decodes his received signals and obtains Alice's messages, it can decide whether to send messages to the receiver Bob with probability  $\eta_R$ . Thus, there are five different cases on the two-hop communications in this work, as illustrated in Fig.2. The probabilities of all cases are given in this figure, which are related to  $\eta_{\scriptscriptstyle A}$  and  $\eta_{\scriptscriptstyle R}.$   $\mathbb{P}_{o,AR}$  is the outage probability on the link between Alice and relay.  $\mathbb{P}_{o,RB}$ is the outage probability on the link between relay and Bob. A red cross x denotes decoding failure, whereas a green checkmark ✓ denotes successful decoding.

Highly directional antennas are commonly utilized in THz communications to overcome significant propagation loss. Therefore, a warden outside the area of a THz signal

beam can hardly observe the signal and perform awfully in detection. Since UAV wardens can wander or hover during detection and we cannot know which mode they work in, we consider the worst scenario for Alice and Bob where UAV wardens hover in the beam area and achieve excellent eavesdropping performance, as shown in Fig.1. Specifically, Willie resides in Alice's signal beam directed to the relay, and Sam resides in the relay's signal beam directed to Bob. Thus, Willie can detect Alice's transmission in the first phase but hardly detect the relay's transmission during the second phase. Similarly, Sam can detect the relay's transmission in the second phase but hardly detect Alice's transmission during the first phase.

#### 3.2. Channel Model

$$\sigma_{tr}^2 = A_{tr,fsp} A_{tr,atm},\tag{1}$$

where  $A_{tr,fsp}$  and  $A_{tr,atm}$  denote the fading of free space propagation and atmospheric attenuation, respectively.

Transmission Probability and Power Optimization for Covert Communications in UAV-Aided THz Wireless Networks

According to the Friis transmission formula, the free space path loss  $A_{tr,fsp}$  can be determined by

$$A_{tr,fsp} = G_t G_r (\frac{c}{4\pi d_{tr} f})^2, \tag{2}$$

where f denotes the carrier frequency and c is the light speed of  $3.0 \times 10^8 \text{m/s}$ .  $G_t$  and  $G_r$  are the antenna gains of the transmitter and receiver, respectively.

Atmospheric attenuation occurs because the wavelength of THz waves is comparable to the size of gaseous molecules, causing resonances at specific carrier frequencies that lead to significant signal degradation. Given that water vapor is the primary contributor to atmospheric attenuation [33], we can approximate the actual attenuation using the attenuation value of water vapor. The expression of atmospheric attenuation is given as

$$A_{tr,atm} = e^{-k(f)d_{tr}}, (3)$$

where k(f) denotes the absorption coefficient of water vapor along the propagation path. We utilize the formula for k(f) as described in [29], which is expressed as

$$k(f) = \frac{0.2205\xi(0.133\xi + 0.0294)}{(0.4093\xi + 0.0925)^2 + (\frac{f}{100c} - 10.835)^2} + \frac{2.014\xi(0.1702\xi + 0.0303)}{(0.537\xi + 0.0956)^2 + (\frac{f}{100c} - 12.664)^2}$$
(4)  
+ 5.54 × 10<sup>-37</sup> f<sup>3</sup> - 3.94 × 10<sup>-25</sup> f<sup>2</sup>  
+ 9.06 × 10<sup>-14</sup> f - 6.36 × 10<sup>-3</sup>,

where  $\xi$  can be calculated by

$$\xi = 6.1121(3.46 \times 10^{-8} \Psi + 1.0007) \frac{\Phi}{\Psi} e^{\frac{17.502 T_C}{240.97 + T_C}}, \quad (5)$$

wherein  $\Phi$  represents the relative humidity in percentage,  $\Psi$  is the pressure in pascal and  $T_C$  is the temperature of Celsius. The main contributing factors of k(f) include the carrier frequency f, the humidity  $\Phi$ , the pressure  $\Psi$  and the temperature  $T_c$ . Obviously, a greater k(f) results in a lower atmospheric attenuation  $A_{Ir,atm}$ , which represents a more severe atmospheric attenuation. Since short-wavelength electromagnetic waves have poor diffraction and penetration capabilities, k(f) becomes greater when f becomes higher. Since water molecules will hinder the propagation of THz radio waves, k(f) becomes greater when  $\Phi$  becomes higher. The pressure and temperature influence the condition and motion of molecules and further influence k(f) and  $A_{tr,atm}$ .

# **3.3.** Noise Model in THz Wireless Communications

In THz wireless communications, receivers experience Johnson-Nyquist noise, resulting from the thermal motion of electrons in conductors. Consistent with [27], the noise power spectral density is denoted as

$$N(f) = \frac{N_f h f}{e^{\frac{h f}{k_B T_K}} - 1},\tag{6}$$

where  $N_f$  represents the noise figure at the receiver, h denotes Planck's constant,  $k_B$  represents the Boltzmann constant, and  $T_K$  indicates the temperature in Kelvin. Consequently, the noise power  $N_r$  at a receiver r is given by  $N_r = \int_W N(f) df$ , where W denotes the bandwidth of THz signals.

#### 3.4. Detection Model of Wardens

In our concerned covert communication scenario, Alice wants to transmit confidential messages to Bob covertly with the help of a UAV relay, whereas "covertly" means that Willie and Sam cannot detect transmissions from Alice and the relay, respectively. The non-colluding wardens perform detections independently, and the detection process of each warden is modeled as hypothesis testing. That is, there are two hypothesis testings in this work, i.e., Willie's hypothesis testing on Alice's transmissions and Sam's hypothesis testing on the relay's transmissions.

In covert communication, prior probabilities represent the probabilities of covert transmissions occurring and not occurring on a link, which are absolute probabilities. Instead of the assumption of "equal prior probabilities" in most existing works, we assume the prior probabilities of covert communications in each hop may be unequal in this work, and define such an assumption as "general prior probabilities". We explain why we do not assume "equal prior probabilities" as below. In this work, we aim to optimize the transmission probabilities of Alice and the relay for the maximum ACT. Different transmission probabilities result in different prior probabilities, thus violating the assumption of "equal prior probabilities". For example, Alice can only transmit with a probability of 0.5 to make  $\mathbb{P}(H_{A,0}) = \mathbb{P}(H_{A,1}) = 0.5$ , where  $H_{A,0}$  represents the null hypothesis that Alice does not transmit signals, and  $H_{A,1}$  represents the alternative hypothesis that Alice transmits signals. Therefore, to study the optimization problem of transmission probabilities in this work, we adopt the assumption of "general prior probabilities" in this work.

Typically, it is difficult for wardens to obtain the correct prior probabilities. Most existing works assume that wardens are unaware of the prior probability of covert transmissions and adopt the hypothesis that wardens assume "equal prior probabilities" for covert communication. However, we cannot rule out the possibility that wardens may possess the correct prior probability. According to [5] and [35], Bash et al. demonstrate that the square root law for covert communication still holds even in scenarios with general prior probabilities, where wardens know the correct prior probabilities and the prior probabilities are general (i.e., may not be equal). The authors also indicate that knowledge of the prior probabilities benefits the warden's detection performance, which makes the wardens more threatening. Therefore, regardless of how wardens acquire this information, if they know or correctly guess the prior probabilities, it represents the worst-case scenario for covert communication. In other words, if covert communication can be achieved against wardens with correct prior probabilities, it Transmission Probability and Power Optimization for Covert Communications in UAV-Aided THz Wireless Networks

can also be achieved against those with unknown or incorrect prior probabilities. Accordingly, in this work, we consider the worst-case scenario for covert communication between Alice and Bob, assuming that Willie and Sam know or have correctly guessed the prior probabilities of covert transmissions by Alice and the relay, respectively. If covert communication can be achieved under such conditions against Willie and Sam, it can likewise be achieved against Willie and Sam with incorrect prior probabilities.

Prior probability and transmission probability are different concepts in this work. As defined above, Alice's transmission probability and relay's transmission probability are denoted as  $\eta_A$  and  $\eta_R$ , respectively. As for prior probabilities of Alice's covert communications (i.e., Alice's transmissions), we define  $\pi_{A,1}$  as the prior probability of  $H_{A,1}$  and  $\pi_{A,0} = 1 - \pi_{A,1}$  as the prior probability of  $H_{A,0}$ . From Fig.2, Alice's transmissions do not exist only in Case 1. Therefore, we can get the prior probabilities of Alice's covert transmissions as

$$\pi_{A,0} = 1 - \eta_A, \pi_{A,1} = \eta_A. \tag{7}$$

Similar to  $\pi_{A,1}$  and  $\pi_{A,0}$ , we denote prior probabilities of relay's covert communications as  $\pi_{R,1}$  and  $\pi_{R,0}$ . From Fig.2, relay's transmissions exist in Cases 4 and 5. Therefore, we can get the prior probabilities of relay's covert transmissions

$$\pi_{R,0} = 1 - \eta_R \eta_A (1 - \mathbb{P}_{o,AR}), \pi_{R,1} = \eta_R \eta_A (1 - \mathbb{P}_{o,AR}). \tag{8}$$

Next, we illustrate the mathematical expression of DEP with the assumption of unequal prior probabilities. As for Willie, he believes that Alice's transmission occurs when the power of his received signals  $P_W$  is not smaller than a

predefined threshold 
$$au_W$$
 and vice versa. That is,  $P_W \mathop{\gtrless}_{H_{A,0}}^{H_{A,1}} au_W$ .

We use  $\mathbb{P}_{FA,W}$  to denote Willie's false-alarm (FA) probability which is the probability of rejecting  $H_{A,0}$  when  $H_{A,0}$ is true, and  $\mathbb{P}_{MD,W}$  to denote Willie's miss-detection (MD) probability which is the probability of rejecting  $H_{A,1}$  when  $H_{A,1}$  is true. According to Bash's PhD thesis [35], Willie's DEP with the assumption of general prior probabilities can be expressed as

$$\mathbb{P}_{e,W} = (1 - \pi_{A,1}) \mathbb{P}_{FA,W} + \pi_{A,1} \mathbb{P}_{MD,W}. \tag{9}$$

And in this case, the covertness constraint is defined as

$$\mathbb{P}_{eW} \ge 0.5 - \epsilon,\tag{10}$$

for any  $\epsilon > 0$ . The detection model of another warden, Sam, is similar to that of Willie and thus is omitted here.

#### 4. Detection Performance Analysis of UTWN

#### 4.1. Detection Error Probability of Willie

Willie detects Alice's transmission signals in the first phase. The received signal  $\mathbf{y}_{w}$  at Willie can be expressed

$$\mathbf{y}_{w} = \left\{ \begin{array}{c} \mathbf{y}_{w,0} = \sqrt{I_{R}} h_{RW} \mathbf{z}_{R} + \mathbf{n}_{w}, & H_{A,0}, \\ \mathbf{y}_{w,1} = \sqrt{P_{A}} h_{AW} \mathbf{x}_{A} + \sqrt{I_{R}} h_{RW} \mathbf{z}_{R} + \mathbf{n}_{w}, & H_{A,1}, \end{array} \right.$$

(11)

where  $\mathbf{x}_A$  is the transmitted signal from Alice,  $\mathbf{z}_R$  is the interference signal from the relay and  $\mathbf{n}_{w}$  is the noise signal received by Willie. Therefore, the power  $P_W$  of  $\mathbf{y}_W$  can be expressed as

$$P_{W} = \begin{cases} P_{W,0} = I_{R}g_{RW} + N_{W}, & H_{A,0}, \\ P_{W,1} = P_{A}g_{AW} + I_{R}g_{RW} + N_{W}, & H_{A,1}. \end{cases}$$
(12)

 $N_W$  is the noise power received at Willie.

When Alice transmits covert messages with a probability of  $\eta_A \in (0, 1]$ , based on (7) and (9), we can express Willie's

$$\mathbb{P}_{e,W} = (1 - \eta_A) \mathbb{P}_{FA,W} + \eta_A \mathbb{P}_{MD,W}. \tag{13}$$

Based on (12), Willie's FA probability is obtained as

$$\mathbb{P}_{FA,W} = \mathbb{P}(g_{RW} \ge \frac{\tau_W - N_W}{I_R} | H_{A,0})$$

$$= \begin{cases} 1, & \tau_W < N_W, \\ e^{-\lambda_2(\tau_W - N_W)}, & \tau_W \ge N_W, \end{cases}$$
where  $\lambda_2 = \frac{1}{2I_R\sigma_{RW}^2}$ .

Willie's MD probability is represented as

$$\mathbb{P}_{M,D,W} = \mathbb{P}(P_A g_{AW} + I_R g_{RW} < \tau_W - N_W | H_{A,1}), (15)$$

where  $g_{AW} \sim \operatorname{Exp}(\frac{1}{2\sigma_{AW}^2})$  and  $g_{RW} \sim \operatorname{Exp}(\frac{1}{2\sigma_{RW}^2})$ . When  $\tau_W < N_W$ , we can simply get that  $\mathbb{P}_{MD,W} = 1$ . When  $\tau_W \geq N_W$ , supposing  $X_1 = P_A g_{AW}$  and  $X_2 = I_R g_{RW}$ , we can know that  $X_1 \sim \operatorname{Exp}(\frac{1}{2P_A\sigma_{AW}^2})$  and  $X_2 \sim \operatorname{Exp}(\frac{1}{2I_R\sigma_{RW}^2})$ . Therefore, defining  $Y = X_1 + X_2$ , the probability density function (PDF) of Y can be calculated as

$$\begin{split} f_{Y}(y) &= \int_{0}^{y} f_{X_{1}}(x_{1}) f_{X_{2}}(y - x_{1}) dx_{1} \\ &= \lambda_{1} \lambda_{2} e^{-\lambda_{2} y} \int_{0}^{y} e^{(\lambda_{2} - \lambda_{1}) x_{1}} dx_{1} \\ &= \begin{cases} \frac{\lambda_{1} \lambda_{2}}{\lambda_{2} - \lambda_{1}} (e^{-\lambda_{1} y} - e^{-\lambda_{2} y}), & \lambda_{1} \neq \lambda_{2}, \\ \lambda^{2} y e^{-\lambda y}, & \lambda_{1} = \lambda_{2} = \lambda, \end{cases} \end{split}$$
(16)

where  $\lambda_1 = \frac{1}{2P_A \sigma_{AW}^2}$ . Then, the CDF of Y is obtained as

$$F_Y(y) = \begin{cases} 1 - \frac{\lambda_2}{\lambda_2 - \lambda_1} e^{-\lambda_1 y} + \frac{\lambda_1}{\lambda_2 - \lambda_1} e^{-\lambda_2 y}, & \lambda_1 \neq \lambda_2, \\ 1 - e^{-\lambda y} (\lambda y + 1), & \lambda_1 = \lambda_2 = \lambda. \end{cases}$$

$$(17)$$

From (15) and (17), we can express  $\mathbb{P}_{MD,W}$  as

$$\begin{split} \mathbb{P}_{MD,W} = & \mathbb{P}(P_{A}g_{AW} + I_{R}g_{RW} < \tau_{W} - N_{W}|H_{A,1}) \\ = & \begin{cases} 0, & \tau_{W} < N_{W}, \\ F_{Y}(\tau_{W} - N_{W}), & \tau_{W} \geq N_{W}. \end{cases} \end{split} \tag{18}$$

Substitute (14) and (18) into (13), we can obtain Willie's

$$\mathbb{P}_{e,W} = \begin{cases} 1 - \eta_A, & \tau_W < N_W, \\ (1 - \eta_A)e^{-\lambda_2(\tau_W - N_W)} + \\ \eta_A F_Y(\tau_W - N_W), & \tau_W \ge N_W. \end{cases}$$
(19)

Transmission Probability and Power Optimization for Covert Communications in UAV-Aided THz Wireless Networks

#### 4.2. Detection Error Probability of Sam

Sam detects forwarding signals from the UAV relay in the second phase. Similar to (9), we can express Sam's DEP as

$$\mathbb{P}_{e,S} = \pi_{R,0} \mathbb{P}_{FA,S} + \pi_{R,1} \mathbb{P}_{MD,S}, \tag{20}$$

where  $\pi_{{\it R},0}$  is the prior probability of  $H_{{\it R},0}$  being true and  $\pi_{R,1} = 1 - \pi_{R,0}$  denotes that of  $H_{R,1}$  being true.  $H_{R,0}$  denotes the null hypothesis that the relay does not transmit signals, and  $H_{R,1}$  denotes the alternative hypothesis against  $H_{R,0}$ , i.e., the relay transmits signals.

When no outage occurs in Alice's transmission, the relay can correctly decode the message and then forward Alice's transmitted information to Bob with a probability of  $\eta_R \in (0,1]$ . Otherwise, the relay can not forward covert information to Bob with a probability of 1. Denoting the SINR of the link between Alice and the relay as  $\gamma_{AB}$ , we can express  $\gamma_{AR}$  as

$$\gamma_{AR} = \frac{P_A g_{AR}}{I_{RR} + N_R},\tag{21}$$

where  $I_{\it RR}$  represents the self-interference generated by the relay on itself. We assume that the relay employs perfect SIC technology to eliminate self-interference, hence  $I_{RR}=0$ . Thus, (21) can be reformulated as  $\gamma_{AR} = P_A g_{AR}/N_R$ .

We define the threshold of SINR for no transmission outage as  $\gamma_{\rm th}$ . Since  $g_{AR} \sim {\rm Exp}(\frac{1}{2\sigma_{AR}^2})$ , the outage probability on the link between Alice and the relay in the first phase can be expressed as

$$\mathbb{P}_{o,AR} = \mathbb{P}(\gamma_{AR} < \gamma_{\text{th}}) = \mathbb{P}(g_{AR} < \frac{\gamma_{\text{th}} N_R}{P_A}) = 1 - e^{-\frac{\gamma_{\text{th}} N_R}{2\sigma_{AR}^2 P_A}}.$$
(22)

Denote the power of Sam's received signals in the second phase as  $P_S$ , we can express it as

$$P_{S} = \left\{ \begin{array}{cc} P_{S,0} = I_{B}g_{BS} + N_{S}, & H_{R,0}, \\ P_{S,1} = P_{R}g_{RS} + I_{B}g_{BS} + N_{S}, & H_{R,1}. \end{array} \right. \tag{23}$$

Similar to (14) and (18), defining  $Z = P_R g_{RS} + I_R g_{RS}$ , we can derive  $\mathbb{P}_{FA,S}$  and  $\mathbb{P}_{MD,S}$  as

$$\mathbb{P}_{FA,S} = \begin{cases} 1, & \tau_S < N_S, \\ e^{-\theta_2(\tau_S - N_S)}, & \tau_S \ge N_S, \end{cases}$$
 (24)

and

$$\mathbb{P}_{MD,S} = \left\{ \begin{array}{cc} 0, & \tau_S < N_S, \\ F_Z(\tau_S - N_S), & \tau_S \geq N_S, \end{array} \right. \eqno(25)$$

where

$$F_Z(z) = \left\{ \begin{array}{cc} 1 - \frac{\theta_2}{\theta_2 - \theta_1} e^{-\theta_1 z} + \frac{\theta_1}{\theta_2 - \theta_1} e^{-\theta_2 z}, & \theta_1 \neq \theta_2, \\ 1 - e^{-\theta z} (\theta z + 1), & \theta_1 = \theta_2 = \theta, \end{array} \right. \tag{26}$$

$$\theta_1 = \frac{1}{2P_R\sigma_{RS}^2}$$
 and  $\theta_2 = \frac{1}{2I_B\sigma_{BS}^2}$ .  $\tau_S$  and  $N_S$  denote the threshold and received noise power at Sam, respectively.

By substituting (8), (22), (24) and (25) into (20), we can derive  $\mathbb{P}_{e,S}$  as

$$\mathbb{P}_{e,S} = \begin{cases} 1 - \delta, & \tau_S < N_S, \\ (1 - \delta)e^{-\theta_2(\tau_S - N_S)} + \\ \delta F_Z(\tau_S - N_S) & \tau_S \ge N_S, \end{cases}$$
(27)

where 
$$\delta = \pi_{R,1} = \eta_R \eta_A e^{-\frac{\gamma_{\rm th} N_R}{2P_A \sigma_{AR}^2}}$$
.

#### 4.3. Infimums of Willie's and Sam's DEPs

We can find that Willie's and Sam's detection threshold significantly influence their DEP, respectively. Since we do not know how much information the adversary has to help the detection of wardens, we opt for a worst-case scenario in covert communication. That is, each warden can apply the optimal threshold to achieve minimum DEP. Since in some cases the DEP only has a lower bound but no minimum, we derive the infimums of Willie's and Sam's DEPs, which include both the minimum and the lower bound in different cases. In this work, we will apply these infimums to measure the overall DEP of non-colluding wardens and further satisfy the covertness constraint with the overall DEP in the optimization problem.

Noting that in Section 3, we describe the assumption that two wardens are located in the main lobe area between the transmitter and receiver of two hops as the worst-case scenario concerning wardens' locations for covert communication. In this subsection, we apply the worst-case scenario for covert communication concerning the threshold selection at wardens in this work, i.e., best threshold for minimal DEP. Both worst-case scenarios for covert communication result in "strong wardens" in this work. As the result, since we explore and achieve covert THz communication with the covertness constraint and throughput maximization against "strong wardens", the theoretical model and optimization framework in this work can still achieve covert communications when the wardens in this work are not "strong wardens", which indicates that this work can serve as a conservative bench mark in the proposed UTWN.

According to (19),  $\mathbb{P}_{e,W}$  remains  $1 - \eta_A$  if  $\tau_W < N_W$ . When  $\tau_W \geq N_W$ , the derivative of  $\mathbb{P}_{e,W}$  with respect to  $\tau_W$ 

$$\frac{\partial \mathbb{P}_{e,W}}{\partial \tau_W} = \begin{cases}
\frac{\eta_A \lambda_1 \lambda_2}{\lambda_2 - \lambda_1} (e^{-\lambda_1 \tau_W'} - e^{-\lambda_2 \tau_W'}) &, \quad \lambda_1 \neq \lambda_2, \\
-\lambda_2 (1 - \eta_A) e^{-\lambda_2 \tau_W'} &, \quad \lambda_1 = \lambda_2 = \lambda, \\
\lambda e^{-\lambda \tau_W'} (\lambda \eta_A \tau_W' + \eta_A - 1), \quad \lambda_1 = \lambda_2 = \lambda,
\end{cases}$$
(28)

where  $F_Z(z) = \left\{ \begin{array}{ll} 1 - \frac{\theta_2}{\theta_2 - \theta_1} e^{-\theta_1 z} + \frac{\theta_1}{\theta_2 - \theta_1} e^{-\theta_2 z}, & \theta_1 \neq \theta_2, \\ 1 - e^{-\theta z} (\theta z + 1), & \theta_1 = \theta_2 = \theta, \end{array} \right. \quad \text{where } \tau_W' = \tau_W - N_W.$  Based on (28), when  $\lambda_1 = \lambda_2 = \lambda$ , we can get the extreme point  $\tau_W^* = \frac{1 - \eta_A}{\lambda \eta_A} + N_W$  and the minimum DEP  $\left( \frac{\eta_A - 1}{\eta_A} \right).$ 

Transmission Probability and Power Optimization for Covert Communications in UAV-Aided THz Wireless Networks

When  $\lambda_1 \neq \lambda_2$ , there are two different cases of  $\mathbb{P}_{e,W}$ . **Case 1**:  $\frac{\lambda_2}{\lambda_1} > \frac{1-2\eta_A}{1-\eta_A}$ . In this case, we can derive the extreme point of  $\mathbb{P}_{e,W}$  as  $\tau_W^* = \frac{1}{\lambda_2 - \lambda_1} \log(1 + \frac{(1-\eta_A)(\lambda_2 - \lambda_1)}{\eta_A \lambda_1}) + N_W$ . The minimum DEP can be obtained as  $\mathbb{P}_{e,W}^* = (1 - \frac{1}{2}) \log(1 + \frac{1}{2}) \log(1 + \frac{1}{2}) \log(1 + \frac{1}{2})$  $\eta_A \kappa_W^{\lambda_2} + \eta_A (1 - \frac{\lambda_2}{\lambda_2 - \lambda_1} \kappa_W^{\lambda_1} + \frac{\lambda_1}{\lambda_2 - \lambda_1} \kappa_W^{\lambda_2})$ , where  $\kappa_W = (1 + \frac{\lambda_2}{\lambda_2 - \lambda_1} \kappa_W^{\lambda_2})$ 

Case 2:  $\frac{\lambda_2}{\lambda_1} \le \frac{1-2\eta_A}{1-\eta_A}$ . In this case, we can find that  $\frac{\partial \mathbb{P}_{e,W}}{\partial \tau_{...}} < 0$  always holds. Thus, the minimum value of  $\mathbb{P}_{e,W}$ does not exist and we can only get a lower bound of  $\mathbb{P}_{e,W}$ . That is,  $\mathbb{P}_{e,W} > \lim_{\tau_W \to +\infty} \mathbb{P}_{e,W} = \eta_A$ .

Considering the two cases above, we use the infimum of DEP to characterize the optimal detection performance of wardens. The infimum of  $\mathbb{P}_{e,W}$  can be expressed as

$$\inf \mathbb{P}_{e,W} = \begin{cases} \eta_A, & \lambda_1 \neq \lambda_2, \frac{\lambda_2}{\lambda_1} \leq \frac{1-2\eta_A}{1-\eta_A}, \\ (1-\eta_A)\kappa_W^{\lambda_2} + \eta_A (1- \frac{\lambda_2\kappa_W^{\lambda_1}}{\lambda_2 - \lambda_1} + \frac{\lambda_1\kappa_W^{\lambda_2}}{\lambda_2 - \lambda_1}), \\ \eta_A (1-e^{\frac{\eta_A-1}{\eta_A}}), & \lambda_1 = \lambda_2 = \lambda. \end{cases}$$

$$\eta_A, & \lambda_1 \neq \lambda_2, \frac{\lambda_2}{\lambda_1} \leq \frac{1-2\eta_A}{1-\eta_A}, \\ T_{RB} \text{ when } g_{AR} \geq \frac{P_RN_Rg_{RB}}{P_AN_B} \text{ and otherwise } T_{AR} < T_{RB}. \text{ The } T_{RB}$$

$$T_{RB} \text{ when } g_{AR} \geq \frac{P_RN_Rg_{RB}}{P_AN_B} \text{ and otherwise } T_{AR} < T_{RB}. \text{ The } T_{RB}$$

$$T_{RB} \text{ when } g_{AR} \geq \frac{P_RN_Rg_{RB}}{P_AN_B} \text{ and otherwise } T_{AR} < T_{RB}. \text{ The } T_{RB}$$

$$T_{RB} \text{ when } g_{AR} \geq \frac{P_RN_Rg_{RB}}{P_AN_B} \text{ and otherwise } T_{AR} < T_{RB}. \text{ The } T_{RB}$$

$$T_{RB} \text{ when } g_{AR} \geq \frac{P_RN_Rg_{RB}}{P_AN_B} \text{ and otherwise } T_{AR} < T_{RB}. \text{ The } T_{RB}$$

$$T_{RB} \text{ when } g_{AR} \geq \frac{P_RN_Rg_{RB}}{P_AN_B} \text{ and otherwise } T_{AR} < T_{RB}. \text{ The } T_{RB}$$

$$T_{RB} \text{ when } g_{AR} \geq \frac{P_RN_Rg_{RB}}{P_AN_B} \text{ and otherwise } T_{AR} < T_{RB}. \text{ The } T_{RB}$$

$$T_{RB} \text{ when } g_{AR} \geq \frac{P_RN_Rg_{RB}}{P_AN_B} \text{ and otherwise } T_{AR} < T_{RB}. \text{ The } T_{RB}$$

Similar to (29), the infimum of Sam's DEP  $\mathbb{P}_{e,S}$  can be derived as

$$\inf \mathbb{P}_{e,S} = \begin{cases} \delta, & \theta_1 \neq \theta_2, \frac{\theta_2}{\theta_1} \leq \frac{1-2\delta}{1-\delta}, \\ (1-\delta)\kappa_S^{\theta_2} + \delta(1-\delta), & \theta_1 \neq \theta_2, \frac{\theta_2}{\theta_1} > \frac{1-2\delta}{1-\delta}, \\ \frac{\theta_2 \kappa_S^{\theta_1}}{\theta_2 - \theta_1} + \frac{\theta_1 \kappa_S^{\theta_2}}{\theta_2 - \theta_1}, & \theta_1 \neq \theta_2, \frac{\theta_2}{\theta_1} > \frac{1-2\delta}{1-\delta}, \\ \delta(1-e^{\frac{\delta-1}{\delta}}), & \theta_1 = \theta_2 = \theta, \end{cases}$$

$$(30)$$

where  $\kappa_S = (1 + \frac{(1 - \delta)(\theta_2 - \theta_1)}{\delta \theta_1})^{\frac{1}{\theta_1 - \theta_1}}$ 

#### 4.4. Overall DEP of Wardens

As stated in [36] and [32], when wardens are noncolluding, they independently detect covert transmissions and know nothing about each other. We need to analyze the strongest warden with the lowest minimum DEP and make the DEP satisfy the covertness constraint (10). Consequently, we can satisfy the covert constraint of each warden. Defining the lowest minimum DEP as  $\mathbb{P}_e$ , we can express it

$$\mathbb{P}_e = \min(\inf \mathbb{P}_{e,W}, \inf \mathbb{P}_{e,S}). \tag{31}$$

#### 4.5. Average Throughput

In this study, the throughput of UTWN refers to the minimum throughput of both hops. The SINRs of transmissions on both hops must not fall below the predefined threshold  $\gamma_{\rm th}.$  That is,  $\gamma_{AR} \geq \gamma_{\rm th}$  and  $\gamma_{RB} \geq \gamma_{\rm th}.$  Therefore,  $g_{AR} \geq \frac{\gamma_{\rm th}N_R}{P_A}$ and  $g_{RB} \ge \frac{\gamma_{\rm th} N_B}{P_R}$ . If the SINR of any hop is smaller than  $\gamma_{\rm th}$ , the throughput becomes zero. Thus, the throughput can be

$$T = \eta_A (1 - \mathbb{P}_{o,AR}) \eta_R (1 - \mathbb{P}_{o,RB}) \min(T_{AR}, T_{RB}), (32)$$

where  $T_{AR}$  and  $T_{RB}$  denote the throughputs of the channel between Alice and the relay and the channel between the relay and Bob, respectively. Similar to (22), we can express the outage probability in the second phase as

$$\mathbb{P}_{o,RB} = \mathbb{P}(\gamma_{RB} < \gamma_{\text{th}}) = \mathbb{P}(g_{RB} < \frac{\gamma_{\text{th}} N_B}{P_R}) = 1 - e^{-\frac{\gamma_{\text{th}} N_B}{2\sigma_{RB}^2 P_R}}.$$
(33)

According to Shannon's formula, we get  $T_{AR} = W \log_2(1 +$  $\gamma_{AR}$ ) and  $T_{RB} = W \log_2(1 + \gamma_{RB})$ . Then we can get  $T_{AR} \ge T_{RB}$  when  $g_{AR} \ge \frac{P_R N_R g_{RB}}{P_A N_B}$  and otherwise  $T_{AR} < T_{RB}$ . The

PDF of 
$$g_{AR}$$
 is  $f_{g_{AR}}(\mu) = \frac{1}{2\sigma_{AR}^2} e^{-\frac{\mu}{2\sigma_{AR}^2}}$  and the PDF of  $g_{RB}$ 

1Hz to get the throughput per unit frequency. The following discussion on throughput will be based on this setting and we derive the average throughput as

$$\begin{split} \overline{T} = & \eta_{A} \eta_{R} \int_{\frac{\gamma_{\text{th}} N_{B}}{P_{R}}}^{+\infty} \int_{\frac{\nu P_{R} N_{R}}{P_{A} N_{B}}}^{+\infty} f_{g_{AR}}(\mu) f_{g_{RB}}(\nu) T_{RB}(\nu) d\mu d\nu + \\ & \eta_{A} \eta_{R} \int_{\frac{\gamma_{\text{th}} N_{B}}{P_{R}}}^{+\infty} \int_{\frac{\gamma_{\text{th}} N_{R}}{P_{A}}}^{\frac{\nu P_{R} N_{R}}{P_{A} N_{B}}} f_{g_{AR}}(\mu) f_{g_{RB}}(\nu) T_{AR}(\mu) d\mu d\nu \\ = & \frac{\eta_{A} \eta_{R}}{\log 2} (e^{-\gamma_{\text{th}}(\zeta_{1} + \zeta_{2})} \log (1 + \gamma_{\text{th}}) - (\zeta_{1} + \zeta_{2})^{-1} \cdot \\ & (\zeta_{1} e^{\zeta_{1} + \zeta_{2}} + \zeta_{2} e^{-\zeta_{1} - \zeta_{2}}) \text{Ei}(-(1 + \gamma_{\text{th}})(\zeta_{1} + \zeta_{2}))), \end{split}$$

$$(34)$$

where  $\zeta_1 = \frac{N_R}{2\sigma_{AR}^2 P_A}$  and  $\zeta_2 = \frac{N_B}{2\sigma_{RB}^2 P_R}$ . The derivation is detailed in Appendix

#### 5. Optimization Problem of Covert **Throughput**

In covert communication, we want to transmit information bits as many as possible while preventing the transmission from being detected. We define ACT as the achieved  $\overline{T}$  while satisfying the covertness constraint. As we stated before, the goal of our optimization problem is to find the optimal values of transmission probabilities and power on both hops that achieve the maximum ACT  $\overline{T}_{\mathrm{cmax}}$ . Thus, the optimization problem can be formulated as

$$\underset{P_A, P_R, \eta_A, \eta_R}{\arg\max} \overline{T}$$
 (35a)

s.t. 
$$\mathbb{P}_e \ge 0.5 - \epsilon$$
, (35b)

Transmission Probability and Power Optimization for Covert Communications in UAV-Aided THz Wireless Networks

$$P_A, P_R \in [0, P_{\text{max}}], \tag{35c}$$

$$\eta_{\scriptscriptstyle A}, \eta_{\scriptscriptstyle R} \in [0, 1], \tag{35d}$$

where  $\epsilon$  is the given parameter representing the strength of covertness constraint and  $\epsilon > 0$ .  $P_{\text{max}}$  is the maximum transmission power of Alice and UAV relay.

The problem (35) is a nonlinear optimization problem with inequality constraints and multiple decision variables. Due to the complexity of (34), it is difficult to obtain the optimal solutions of (35) and the closed-form expression of the maximum ACT. In this work, we apply a heuristic method named genetic algorithm (GA) to solve (35), which is available for various kinds of optimization problems. We design and implement the method as Algorithm 1. Considering the principle of GA and the discrete sampling of a continuous solution space, it is very likely that we get a near-optimal solution for ACT maximization by Algorithm 1. The key concepts and operations of Algorithm 1 are illustrated as follows.

```
Algorithm 1: GA for the solution of (35)
```

**Input:**  $\epsilon$ : Strength of covertness constraint; **Output:**  $P_A^*$ ,  $P_R^*$ ,  $\eta_A^*$ ,  $\eta_R^*$ : Optimal values of  $P_A$ ,  $P_R$ ,  $\eta_A$  and  $\eta_R$  which achieve maximum ACT;  $\overline{T}_{\text{cmax}}$ : Maximum ACT;

- 1 Initialization: Maximum generations K, population size N, crossover probability  $p_c$ , mutation probability  $p_m$ ;
- 2 Randomly generate the initial population with genes;
- 3 Calculate the fitness scores of the population according to the fitness function  $F_{fit}$  and record the scores;

```
4 k = 1;
5 for k \le K do
```

6 | Select individuals from the previous population;

Generate offspring by crossover with a preset probability  $p_c$ ;

8 Mutate offspring with a preset probability  $p_m$ ;

Offspring constitute the new generation of population;

Calculate the fitness score of the population and record the score;

Store the gene of the individual with the highest fitness score and record the score as  $\overline{T}_{\rm cmax}$ ;

if termination criteria are satisfied then

13 break;

14 end

15 end

10

11

12

16 Obtain  $P_A^*$ ,  $P_R^*$ ,  $\eta_A^*$  and  $\eta_R^*$  by translating the gene of the best individual.

**Genotype**: In (35),  $P_A$ ,  $P_R$ ,  $\eta_A$  and  $\eta_R$  are decision variables, and each of them is represented by 8 consecutive binary numbers. Then, the genotype consists of 32 binary numbers.

**Fitness function**: The fitness function gives an individual's fitness score based on its gene, indicating their environmental adaptability. The fitness function of our problem is defined as

$$F_{fit} = \begin{cases} 0, & \mathbb{P}_e < 0.5 - \epsilon, \\ \overline{C}, & \mathbb{P}_e \ge 0.5 - \epsilon. \end{cases}$$
 (36)

**Selection**: In each generation, we use the tournament selection method to select individuals from the population of the last generation based on their fitness scores and obtain a new population. An individual with a higher fitness score is more likely to be selected and remain in the population.

**Crossover**: The population will give birth to offspring with a preset probability  $p_c$ , and the offspring's genes are formed by the crossover of their parents' genes. Otherwise, the crossover will not occur, and the offspring's genes will be the same as their parents.

**Mutation**: Once a new individual is generated, it mutates with a preset probability  $p_m$ . Once it mutates, a random binary number in its gene will be inverted. That is, 0 becomes 1, and 1 becomes 0. After selection, crossover, and mutation, all offspring form a new population generation.

**Termination criteria**: The iterations in Algorithm 1 are terminated if the genes of the best individual remain unchanged after a specified number of generations, or if the maximum number of generations has been reached.

#### 6. Numerical Results

We first obtain the numerical results of Willie's DEP, Sam's DEP, and average throughput, and then give the simulation results to validate our derivations. Then, we implement Algorithm 1 in Matlab to get the optimal values of decision variables for maximum ACT in problem (35), and acquire the numerical results to explore the impacts of critical parameters on network performance. Based on these results, we further analyze the prior probabilities of Alice's and the relay's covert transmissions and get a meaningful finding. Unless otherwise specified, the values of main parameters are listed in Table 2. Besides, we set the distances of links as  $d_{AR}=100$ m,  $d_{RB}=150$ m,  $d_{AW}=60$ m,  $d_{RW}=40$ m,  $d_{RS}=80$ m and  $d_{BS}=70$ m. As for figures illustrating the results of GA, we execute Algorithm 1 once for each point on the horizontal axis, including the initialization, evolution, and convergence of the population. By setting a sufficiently large population size and maximum iteration number, as well as setting high crossover and mutation probabilities, the exploration ability of GA can be effectively guaranteed, thereby improving the reliability of solutions obtained by executing GA once. On the other hand, under the premise that the concealment constraint is always satisfied, although the curves of the decision parameters obtained by executing GA once fluctuate in Fig.10, Fig.12 and Fig.14, the stability exhibited by the curves of maximum ACT (smoothness of the curves) in Fig.9, Fig.11, and Fig.13 indicates that the optimization result obtained by running GA once is effective and stable with a reasonable configuration of algorithm parameters.

Transmission Probability and Power Optimization for Covert Communications in UAV-Aided THz Wireless Networks

**Table 2**Main Parameters

Parameter name	Value
Carrier frequency	300GHz
Subcarrier bandwidth	5GHz
Maximum transmission power	1W
SINR threshold	20dB
Antenna gain	27dB
Noise figure	1
Population size in GA	10000
Maximal generations in GA	1000
Crossover probability in GA	0.6
Mutation probability in GA	0.5

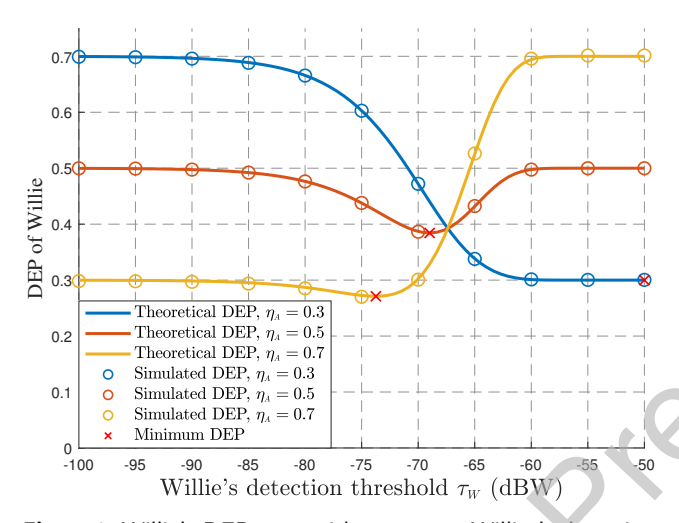
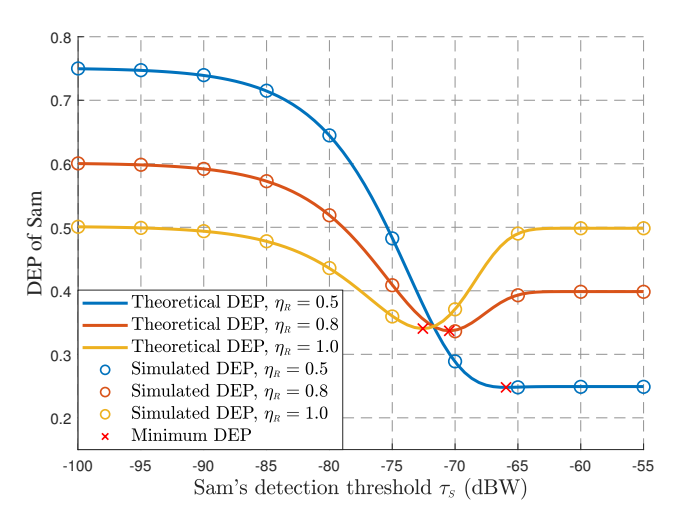


Figure 3: Willie's DEP  $\mathbb{P}_{e,W}$  with respect to Willies's detection threshold  $\tau_W$  for different Alice's transmission probability  $\eta_A$  when  $P_A = I_R = 0.1 W$ .

#### 6.1. Validation of DEP and Average Throughput

We first explore the impact of  $\eta_A$  on Willie's DEP  $\mathbb{P}_{e,W}$ . As illustrated in Fig.3, when  $\eta_A = 0.3$  or  $\eta_A = 0.7$ , although Willie's DEP will become very high when  $\tau_W$  is in a specific interval, there is another interval of  $\tau_w$  that makes the DEP very low. The minimum DEP of Willie is higher when  $\eta_A = 0.5$  compared to  $\eta_A = 0.3$  and  $\eta_A = 0.7$ . Note that when  $\eta_A = 0.3$ , there is no minimum value of  $\mathbb{P}_{e,W}$ , but only the limit value as a lower bound when  $\tau_W$  tends to positive infinity. For ease of comparison, we draw a point of (-50, 0.3) as Willie's minimum DEP with  $\eta_A = 0.3$ , as shown in Fig.3. Although we do not show the impacts of  $P_A$  and  $I_R$  on  $\mathbb{P}_{e,W}$ , we can easily find that  $\mathbb{P}_{e,W}$  becomes lower with a larger  $P_A$  or a smaller  $I_R$  as illustrated in our work [30]. It is reasonable since more powerful signals are easier to detect, and stronger interference helps hide covert signals. Simulation results verify the correctness of (19). Meanwhile, we also calculate Willie's minimum DEP with optimal thresholds based on (29) and mark the points in Fig.3. We can see that these points match the curves, which illustrate the correctness of our derivation. In addition,  $\eta_A$ 



**Figure 4:** Sam's DEP  $\mathbb{P}_{e,S}$  with respect to Sam's detection threshold  $\tau_S$  for different relay's transmission probability  $\eta_R$  when  $\eta_A=0.5$  and  $P_A=P_R=I_R=I_B=0.1W$ .

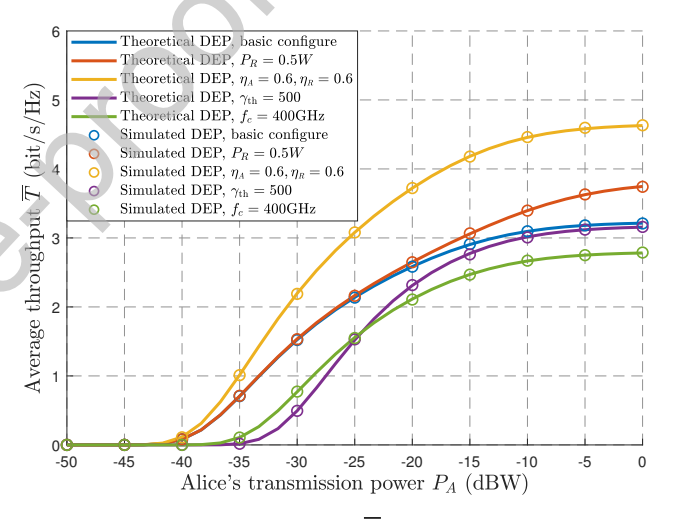


**Figure 5:** Average throughput  $\overline{T}$  with different values of configure parameters.

achieves the biggest value of Willie's minimum DEP, which deteriorates Willie's detection.

In Fig.4, the pattern between  $\eta_R$  and  $\mathbb{P}_{e,S}$  when  $\eta_A=0.5$  and  $P_A=P_R=I_R=I_B=0.1W$  is shown. When  $\eta_R=0.5$ , Sam's DEP is large when  $\tau_S$  is in a specific interval, while there is another interval of  $\tau_S$  that makes the DEP small. Among the three curves, we can find that the minimum DEP of  $\eta_R=1.0$  is higher than those of  $\eta_R=0.5$  and  $\eta_R=0.8$ , and minimum DEPs of  $\eta_R=0.8$  and  $\eta_R=1.0$  are very close. Therefore, compared to the impact of  $\eta_A$  on  $\mathbb{P}_{e,W}$ ,  $\eta_R$  has a weaker influence on  $\mathbb{P}_{e,S}$ .

The theoretical values of average throughput  $\overline{T}$  and corresponding simulation results with different values of critical parameters are shown in Fig.5. Note that the curves of  $\overline{T}$  are respect to  $P_A$  and the basic config consists of  $P_R=0.1W$ ,  $\eta_A=\eta_R=0.5$ ,  $\gamma_{\rm th}=100$  and  $f_c=300{\rm GHz}$ . The legend of this figure illustrates the inconsistent parameters for curves with a different value of one parameter compared to the basic

Transmission Probability and Power Optimization for Covert Communications in UAV-Aided THz Wireless Networks

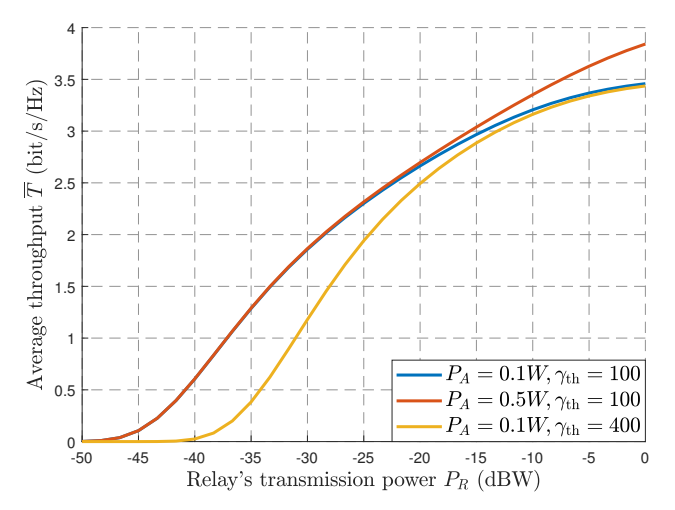


**Figure 6:** Average throughput  $\overline{T}$  for different relay's transmission power  $P_R$  when  $\eta_A = \eta_R = 0.5$ .

config. From Fig.5, we can see that  $\overline{T}$  becomes bigger when both  $\eta_A$  and  $\eta_R$  become higher since higher transmission probabilities mean more chances to send signals and make a larger throughput. A bigger threshold of SINR results in a lower  $\overline{T}$  because the requirement of wireless communication becomes stricter. Besides,  $\overline{T}$  is restricted by  $P_A$  when  $P_A$  is less than a certain value since the throughput of the first hop is smaller than that of the second hop, and vice versa. Moreover, we find that  $\overline{T}$  with the carrier frequency  $f_c = 400 \, \mathrm{GHz}$  is less than that with  $f_c = 300 \, \mathrm{GHz}$ . This is due to a more severe propagation loss caused by a higher  $f_c$ . Besides, simulation results show the correctness of (34).

# **6.2.** Impacts of Decision Parameters on Average Throughput

In this subsection, we will further discuss the impacts of decision parameters on average throughput  $\overline{T}$ . Since the impact of  $P_A$  is already shown in Fig.5, we first illustrate the impact of  $P_R$  in Fig.6. We can see that  $\overline{T}$  grows with the increase of  $P_R$ , and the growth speed becomes faster first and then slows down gradually. Meanwhile, we can also find that when  $P_R$  is small,  $\overline{T}$  of  $P_A = 0.1W$  is the same as  $\overline{T}$  of  $P_A = 0.5W$  when  $\gamma_{\rm th} = 100$ . Because  $\overline{T}$  is the minimal average throughput of two hops and a small  $P_R$  makes  $\overline{T}_{RB}$  less than  $\overline{T}_{AR}$ . Thus, if  $P_A$  is sufficiently larger than  $P_R$ ,  $\overline{T}$  does not change with different  $P_A$ .

When  $P_R$  is large resulting  $\overline{T}_{RB} \geq \overline{T}_{AR}$ , we can obtain  $\overline{T} = \overline{T}_{AR}$  and  $\overline{T}_{AR}$  is related to  $P_A$ . Therefore, we can see that  $\overline{T}$  of  $P_A = 0.5W$  is larger than  $\overline{T}$  of  $P_A = 0.1W$  when  $\gamma_{\rm th} = 100$ , and  $\overline{T}$  of  $\gamma_{\rm th} = 100$  is close to  $\overline{T}$  of  $\gamma_{\rm th} = 400$  when  $P_A = 0.1W$  with a large  $P_R$  in Fig.6.

The pattern between  $\overline{T}$  and  $\eta_A$  is illustrated in Fig.7. Regardless of the values of  $P_A$  and  $P_R$ ,  $\overline{T}$  and  $\eta_A$  show a positive correlation, as shown in Fig.7. This rule can be proved by (34). In Fig.8, the impact of  $\gamma_{th}$  on  $\overline{T}$  is shown. Naturally, the larger  $\gamma_{th}$  is, the smaller  $\overline{T}$  is. Besides, an equal

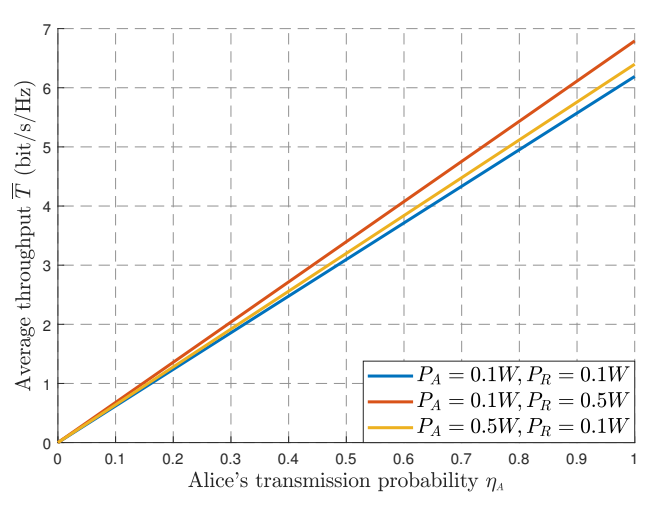
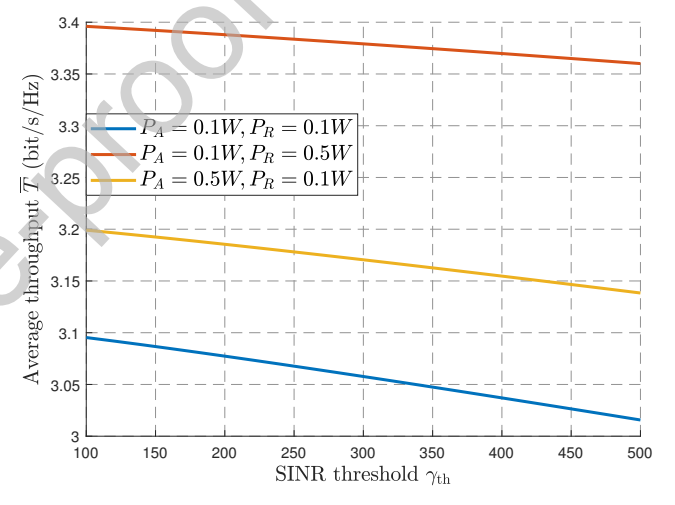


Figure 7: Average throughput  $\overline{T}$  for different Alice's transmission probability  $\eta_A$  when  $\eta_R=0.5$ .



**Figure 8:** Average throughput  $\overline{T}$  for different SINR threshold  $\gamma_{\rm th}$  when  $\eta_A = \eta_R = 0.5$ .

increase in  $P_R$  can result in a higher  $\overline{T}$  than  $P_A$ , which can be found in Fig.7 and Fig.8.

# **6.3.** Impacts of Decision Parameters on Maximum ACT

The optimization of maximum ACT  $\overline{T}_{cmax}$  is formulated regarding the transmission power and transmission probabilities of both hops in the proposed UTWN. To solve this problem, we design Algorithm 1 based on GA to obtain optimal values of  $P_A$ ,  $P_R$ ,  $\eta_A$  and  $\eta_R$  which achieve  $\overline{T}_{cmax}$  with a given  $\epsilon$ . By Algorithm 1, we obtain  $\overline{T}_{cmax}$  for different  $\epsilon$  and illustrate it in Fig.9. For  $I_B = I_R = 0.1W$ ,  $\overline{T}_{cmax}$  equals 0 when  $\epsilon \leq 0.01$ ; for  $I_B = I_R = 0.01W$ ,  $\overline{T}_{cmax}$  equals 0 when  $\epsilon \leq 0.05$ . The reason why  $\overline{T}_{cmax}$  equals 0 is that the covertness constraint is too strong to be satisfied (i.e., small  $\epsilon$ ) with the given interference power. When the constraint is satisfied,  $\overline{T}_{cmax}$  becomes larger with stronger interference because it helps cover the signals. Meanwhile,

Transmission Probability and Power Optimization for Covert Communications in UAV-Aided THz Wireless Networks

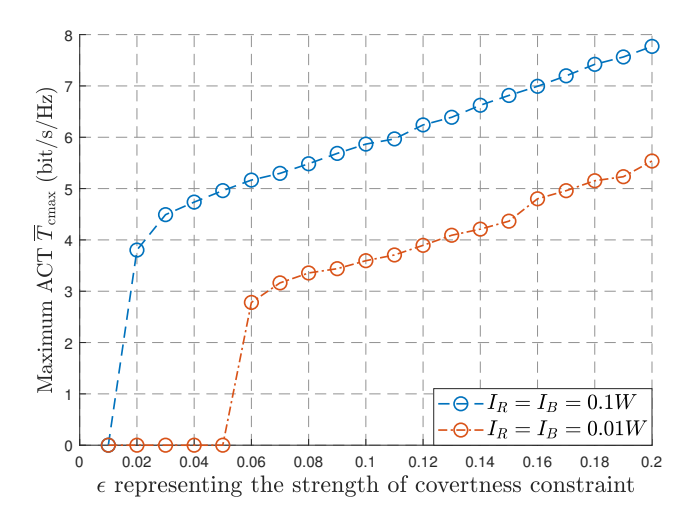
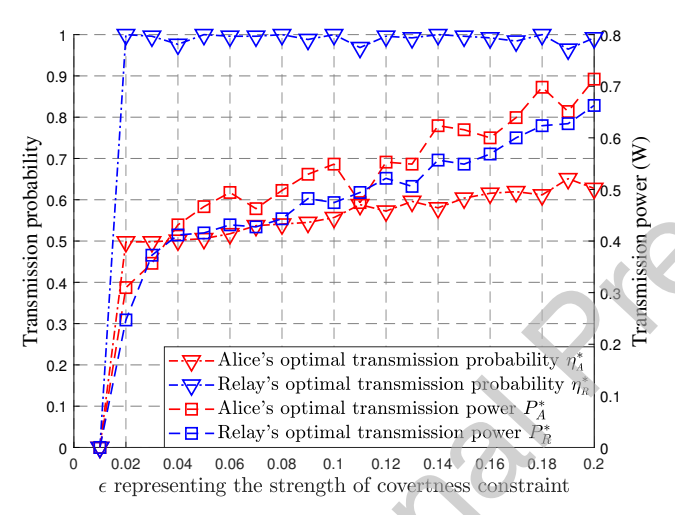


Figure 9: Maximum average covert throughput (ACT)  $\overline{T}_{\rm cmax}$  for different  $\epsilon$  representing different strength of covertness constraint



**Figure 10:** Optimal decision parameters  $P_A^*, P_R^*, \eta_A^*$  and  $\eta_R^*$  to achieve  $\overline{T}_{\rm cmax}$  for different  $\epsilon$  when  $I_B=I_R=0.1W$ .

 $\overline{T}_{\rm cmax}$  shows an approximately positive linear relationship with respect to  $\epsilon$  since we can transmit signals with a higher power while keeping the signals covert with a large  $\epsilon$ . More information bits can be delivered covertly when the covertness constraint is weaker.

Fig. 10 shows the optimal decision parameters  $P_A^*$ ,  $P_R^*$ ,  $\eta_A^*$  and  $\eta_R^*$  to achieve  $\overline{T}_{\rm cmax}$  for different  $\epsilon$  when  $I_R=I_B=0.1W$  in Fig.9. As illustrated in Fig.10, all these parameters equal 0 for small  $\epsilon \leq 0.01$  since we cannot satisfy the covertness constraint and thus do not emit covert signals. When  $\epsilon >= 0.02$ ,  $P_A^*$  and  $P_R^*$  show a growing trend as  $\epsilon$  increase. The trend fits the growing trend of  $\overline{T}_{\rm cmax}$  in Fig.9. Meanwhile,  $\eta_R^*$  is always close to 1.0, and  $\eta_A^*$  increases with the increase of  $\epsilon$ . It means that, given a larger  $\epsilon$  and predefined parameters in the network, Alice can transmit signals with a higher  $\eta_A$  and the relay always needs to forward the messages once it receives Alice's signals and successfully decodes them. This phenomenon occurs because when  $\epsilon$  is

large, the covertness constraint can be satisfied even if the transmission probability is high. Besides, the phenomenon also indicates that compared to  $\eta_R$ ,  $\eta_A$  takes a more significant influence on  $\overline{T}_{\rm cmax}$ .

Noting that the curves of  $P_A^*$ ,  $P_R^*$ ,  $\eta_A^*$  and  $\eta_R^*$  has small fluctuations. Generally, a larger  $\epsilon$  refers to a weak covertness constraint and thus results in a larger transmission probability in covert communication. But in Fig.10, sometimes both  $P_A^*$  and  $P_R^*$  decrease with a larger  $\epsilon$ . In this case, we can see that  $\eta_{\scriptscriptstyle A}^*$  will increase and finally enlarge  $\overline{T}_{\rm cmax}$ . Therefore, the decrease of  $P_A^*$  and  $P_R^*$  is not unreasonable if a higher  $\overline{T}_{\rm cmax}$  can be achieved. As for the fluctuations, we come up with two potential reasons. First, GA may converge to different solutions over multiple simulations with the same configuration. For each  $\epsilon$ , GA will reinitialize the population and search for the optimal solution. The exploration and mutation of GA is also random. Therefore, the convergence process (the process of finding the best individual in the solution space) is uncertain, resulting in different solutions. If the fitness values corresponding to multiple alternative solutions are very close, GA may obtain a random solution among these alternative solutions. Consequently, the obtained solution with a given  $\epsilon$  may not be adjacent enough to the solution obtained with adjacent  $\epsilon$ , which results in fluctuations. Another reason is that the resolution of GA is not small enough. The length of gene sequence determines the resolution of decision variables, and a long length represents a small resolution which reduces the errors of adjacent sample values of a decision variable. If the resolution is not small enough, errors between obtained solutions and real optimal solution are large, which results in fluctuations of curves in Fig.10. Regardless of these reasons, the curves of  $T_{\rm cmax}$  in Fig.9, 11, and 13 are approximately smooth, which verifies the effectiveness of Algorithm 1 in obtaining optimal decision parameters and achieving  $T_{\rm cmax}$ . This phenomenon also indicates that there is a subspace in the solution space where multiple alternative solutions can achieve very similar ACT. Algorithm 1 may converge to a random alternative solution in this subspace and the randomness could result in the fluctuations in Fig.10.

Fig.11. illustrates the impact of interference power on  $\overline{T}_{\rm cmax}$ . Here, inference power is the values of  $I_R$  and  $I_B$  and we set  $I_B=I_R$ . As the interference power increases,  $\overline{T}_{\rm cmax}$  also increases and the growth rate is slowing down. Meanwhile, a lower  $\epsilon$  results in a smaller  $\overline{T}_{\rm cmax}$ . The values of  $\overline{T}_{\rm cmax}$  with  $\epsilon=0.1$  and  $\epsilon=0.05$  when  $I_R=I_B=0.1W$  in Fig.11 also match the values in Fig.9.

The optimal decision parameters  $P_A^*$ ,  $P_R^*$ ,  $\eta_A^*$  and  $\eta_R^*$  to achieve  $\overline{T}_{\rm cmax}$  for different interference power when  $\epsilon=0.1$  and  $I_R=I_B=0.1W$  are shown in Fig.12. As the interference power increases,  $\eta_A^*$  continues to grow slightly and  $\eta_R^*$  remains almost unchanged when the interference power is larger than 0.5W. Meanwhile,  $P_A^*$  and  $P_R^*$  also increase in most cases, and the fluctuations of curves can be explained as above. It means that higher transmission power

Transmission Probability and Power Optimization for Covert Communications in UAV-Aided THz Wireless Networks

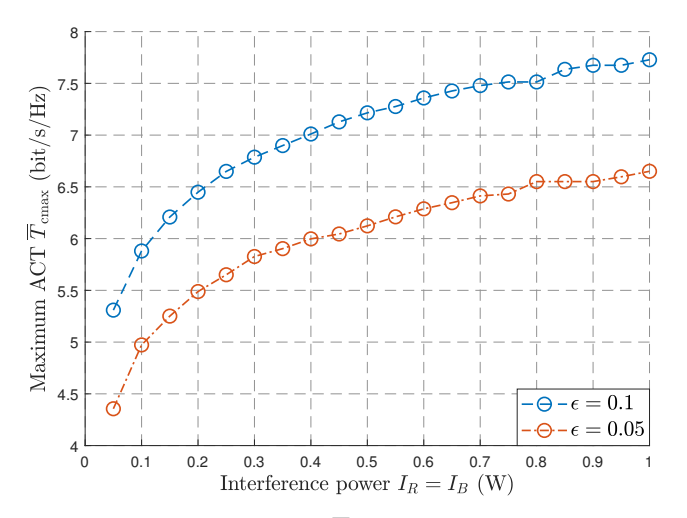


**Figure 11:** Maximum ACT  $\overline{T}_{\rm cmax}$  for different interference power  $I_R = I_B$ .

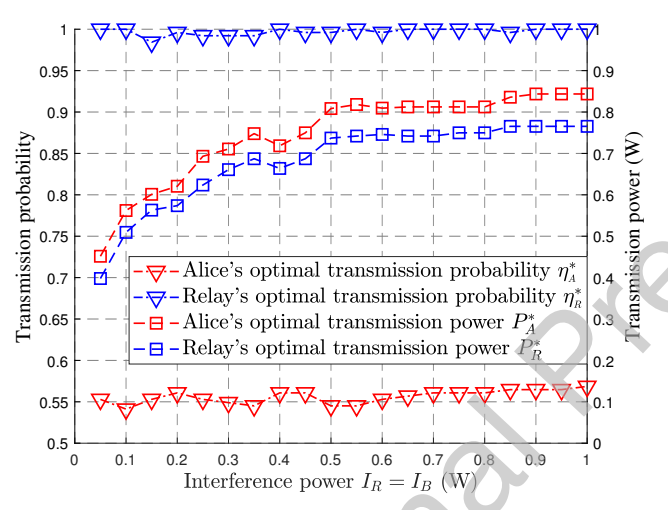


**Figure 12:** Optimal decision parameters  $P_A^*$ ,  $P_R^*$ ,  $\eta_A^*$  and  $\eta_R^*$  to achieve  $\overline{T}_{\rm cmax}$  for different interference power when  $\epsilon=0.1$ .

in two hops can also satisfy the covertness constraint with the help of larger interference, thus enhancing  $\overline{T}_{\rm cmax}$ .

 $\overline{T}_{cmax}$  for different  $P_{max}$  when  $I_R = I_B = 0.1 W$  is shown in Fig.13. When  $P_{max}$  is smaller than a specific value,  $\overline{T}_{cmax}$  increases with the increase of  $P_{max}$ . We can find the reason in Fig.14, in which  $P_A^*$ ,  $P_R^*$ ,  $\eta_A^*$  and  $\eta_R^*$  for  $\overline{T}_{cmax}$  when  $\epsilon = 0.1$  are illustrated. Please note that  $\eta_A^*$  and  $\eta_R^*$  represent Alice's optimal transmission probability and the relay's optimal transmission probability, respectively, and they are distinct from the concept of prior probabilities. Their differences have been explained in detail in Section 3.4. Actually, greater  $P_A$  and  $P_R$  than  $P_A^*$  and  $P_R^*$  can also satisfy the covertness constraint, but a small  $P_{max}$  limits the transmission power in two hops. Therefore,  $P_A^*$  and  $P_R^*$  are just the same as  $P_{max}$  when  $P_{max}$  is small as shown in Fig.14. Besides,  $\eta_A^*$  firstly remains close to 0.6 and then falls to 0.55, while  $\eta_R^*$  is always close to 1. It is because a larger  $\eta_A^*$  with a small  $P_A^*$  and  $P_R^*$  can still satisfy the covertness constraint

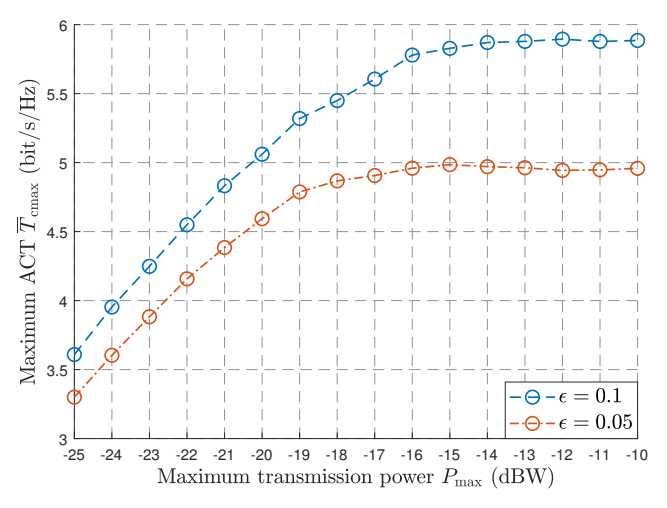
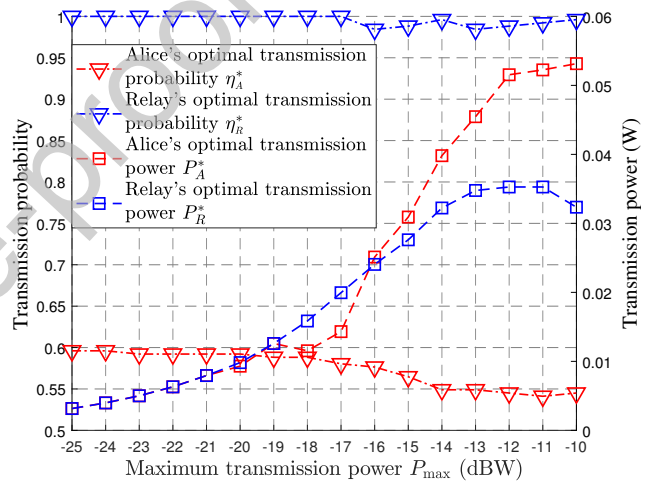


Figure 13: Maximum ACT  $\overline{T}_{\rm cmax}$  for different maximum transmit power  $P_{\rm max}$  when  $I_R=I_B=0.1W$  .



**Figure 14:** Optimal decision parameters  $P_A^*, P_R^*, \eta_A^*$  and  $\eta_R^*$  to achieve  $\overline{T}_{\rm cmax}$  for different  $P_{\rm max}$  when  $\epsilon=0.1$  and  $I_B=I_R=0.1W$ .

and achieve  $\overline{T}_{\rm cmax}$ . When  $P_{\rm max}$  becomes large enough, the limitation of  $P_A^*$  and  $P_R^*$  disappear. We can see that  $\overline{T}_{\rm cmax}$  remains almost unchanged at the right side of curves in Fig.13.

# **6.4.** Prior Probabilities of Transmissions in the UTWN When Maximum ACT Is Achieved

As we stated above, the prior probability  $\pi_{A,1}$  of Alice's transmission represents the probability of  $H_{A,1}$  being true, i.e., the probability of the existence of Alice's transmission. Similarly,  $\pi_{R,1}$  represents the probability of  $H_{R,1}$  being true. Fig.15 shows the values of  $\pi_{A,1}$  and  $\pi_{R,1}$  for different  $\epsilon$  when  $\overline{T}_{\text{cmax}}$  is achieved. We do not show  $\pi_{A,0}$  and  $\pi_{R,0}$  in Fig.15 since  $\pi_{A,0} = 1 - \pi_{A,1} = \text{and } \pi_{R,0} = 1 - \pi_{R,1}$ . This figure illustrates that both  $\pi_{A,1}$  and  $\pi_{R,1}$  equal 0 when  $\epsilon = 0.01$  since the covertness constraint cannot be satisfied with given network parameters, and thus, no covert transmission occurs.

Transmission Probability and Power Optimization for Covert Communications in UAV-Aided THz Wireless Networks

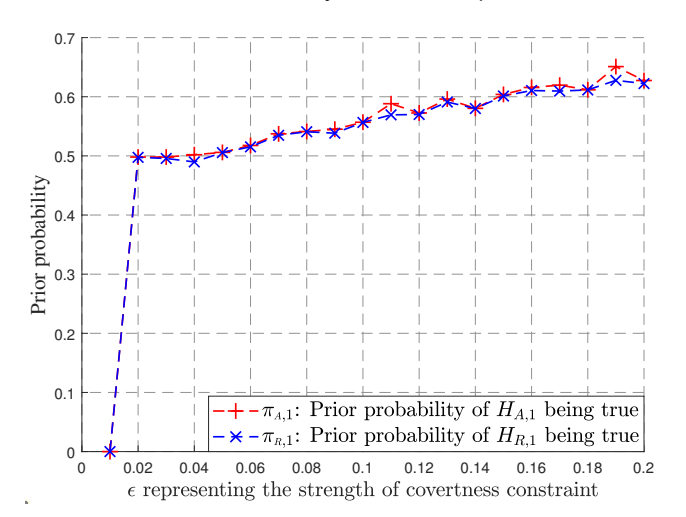


**Figure 15:** Prior probabilities  $\pi_{\scriptscriptstyle A,1}$  and  $\pi_{\scriptscriptstyle R,1}$  when  $\overline{T}_{\scriptscriptstyle \rm cmax}$  is achieved for different  $\epsilon$  with  $I_{\scriptscriptstyle B}=I_{\scriptscriptstyle R}=0.1W$ .

We can see that  $\pi_{A,1}$  and  $\pi_{R,1}$  are close to 0.5 when  $0.02 \le$  $\epsilon \leq 0.05$ . When  $\epsilon \geq 0.06$ ,  $\pi_{A,1}$  and  $\pi_{R,1}$  show a growing trend while  $\epsilon$  is increasing. In this case, both  $\pi_{A,1}$  and  $\pi_{R,1}$ are greater than 0.5. This result indicates that equal prior probabilities are not always the optimal selection for multihop covert communication, especially for a large  $\epsilon$ . Accordingly, the assumption of equal prior probabilities at wardens may not be reasonable since Alice and relay can apply unequal prior probabilities and achieve optimal performance. Furthermore, even if wardens have a priori knowledge of the prior probabilities of transmissions, the minimum overall DEP  $\mathbb{P}_{\mathfrak{a}}$  we derive is the optimal detection performance that wardens can theoretically achieve. Research on performance optimization of covert communication needs further discussion and verification with the assumption about "general prior probabilities". For the design and implementation of covert communication systems, the control of transmission probability and the adjustment of prior probability need to be carefully considered to achieve more accurate and realistic optimal covert communication performance. For wardens, research on their knowledge of prior probabilities and their strategies of setting prior probabilities is still absent, which needs further consideration and discussion in covert communication. These findings illustrate the significance of our research.

# 7. Discussion of Practical Challenges and Implementation Considerations

We will mainly discuss the practical challenges and implementation considerations of this work in application from three aspects: mobility, coordination, and overhead.

#### 7.1. Mobility

In wireless communications, communication nodes often exhibit mobility. Numerous techniques and schemes have been proposed and designed to maintain the stability of mobile communications. However, this significantly increases the complexity of communication systems, especially when the system has specific requirements.

This work focuses on covert communication in a UAV-assisted two-hop system operating in the THz band. First, THz communication is currently in the experimental stage and has not yet been widely commercialized. Furthermore, due to the severe propagation loss of THz signals in the air, THz wireless communications impose higher demands on antennas, such as high directivity and beam tracking capabilities. Additionally, the requirement for signal covertness makes covert communication particularly sensitive to environmental conditions.

Considering these factors, this work assumes that the ground nodes, such as Alice and Bob, are stationary, and the position of the UAV relay is pre-determined based on CSI and geographical data, with the relay operating in a hovering mode. As a result, the network topology is stable, which helps maintain system performance, reduces the complexity of the covert communication system, and facilitates practical implementation.

#### 7.2. Coordination

We will introduce some coordination mechanisms in the considered network to illustrate how to apply the network and optimization framework studied in this work in reality. The hovering position of the UAV relay can be obtained based on geographic and topographic data and CSI, while the CSI can be obtained by pilot signals. The covertness of pilot signals has been explored in [37, 38]. Alice and the relay can also know whether a warden is located in the signal beam or not by sensing techniques, and existing works have also discussed such technologies [39, 40]. The principles and technologies of how to prevent sensing signals (or radar signals) from being intercepted are well studied and discussed [41].

We assume that Alice is a ground communication node with sufficient computational capability. Based on environmental and algorithmic parameters, the optimal transmission power and transmission probabilities for both Alice and the relay are obtained by applying the proposed optimization framework. The optimized parameters for the relay are sent from Alice to the relay via pilot signals. The relay and Bob set a fixed interference power based on the estimation of their own battery capacity and power consumption.

#### 7.3. Overhead

GA is a widely applicable heuristic optimization method. The algorithm parameters must be carefully tuned according to the specific problem context. The computational cost of GA is primarily influenced by three factors: the gene length of each individual, the population size, and the overhead of fitness evaluation. In this work, each decision variable is represented by an 8-bit binary sequence. We choose this value to balance solution precision and computational cost. The population size is selected to ensure strong exploratory capability under a single run of GA. The cost of fitness evaluation is determined by the complexity involved in computing the DEP and the ACT. Furthermore, the computational

Transmission Probability and Power Optimization for Covert Communications in UAV-Aided THz Wireless Networks

overhead can be reduced through parallel programming and approximate calculation of the mathematical expressions. In this way, we can control the overhead of GA to an acceptable level and apply it to practical scenarios.

As for the power consumption of the network, since the optimization problem incorporates constraints on the maximum transmission power and employs fixed interference power, the overall power consumption remains controllable.

#### 8. Conclusion

This paper investigates the covert THz communication by joint transmission probability and power optimization in a UTWN against two UAV wardens. Unlike most existing works, which assume equal prior probabilities at transmitters, we derive the overall DEP of non-colluding wardens based on general prior probabilities considering the transmission probability and outage probability. We also assume that wardens know or correctly guess the prior probabilities of covert transmissions in two hops and achieve high detection accuracy, which is the worst-case scenario for covert communication. To investigate the impacts of the transmission power and transmission probabilities at Alice and the UAV relay on maximum ACT, we solve the optimization problem with a GA-based optimization algorithm. Numerical and simulation results are presented to validate our theoretical analysis and also to illustrate our findings.

Particularly, we find that prior probabilities of transmissions in each hop may be unequal when the maximal ACT is achieved. For a weak covertness constraint (a large  $\epsilon$ ), the probability of the existence of covert transmission could be greater than 0.5 to achieve maximum ACT. This suggests that the performance analysis of covert communication should consider scenarios with the assumption of general prior probabilities, and wardens may achieve the best detection performance by applying correct prior probabilities in hypothesis testing. Therefore, it is important to study the transmission probabilities of the source and relays in multi-hop communication networks, since transmission probabilities significantly influence prior probabilities and the detection performance of wardens. In future research, we aim to tackle the joint optimization problem against colluding wardens in the proposed UTWN to protect wireless transmissions from stronger adversaries. Additionally, we will jointly consider transmission power and probability, as well as cooperative interference power, for covert performance optimization in the network. In order to solve optimization problems with many decision parameters quickly, algorithms with faster convergence need to be considered and designed.

#### Acknowledgments

This work is supported in part by the National Natural Science Foundation of China under Grant No. 62372076; in part by the Japan Society for the Promotion of Science under Grant No. 23K28076; in part by the Education Department Research Foundation of Anhui Province under Grant

No. DTR2023051, 2023AH051593 and 2022AH051097; in part by the Innovation Research Team on Future Network Technology of Chuzhou University; in part by the Innovation Team on Smart Home Appliance Security and Applications of Chuzhou City; in part by the Innovative Research Team on Application of Big Data and Financial Technology of Chuzhou University.

### A. Derivation of the Average Throughput $\overline{T}$

We detail the derivation of  $\overline{T}$  in this appendix. Denoting  $k_1 = \frac{\gamma_{\text{th}} N_B}{P_R}$  and  $k_2 = \frac{P_R N_R}{P_A N_B}$ , the derivation of first integral in (34) is given as

$$\begin{split} &\int_{\frac{\gamma_{\text{th}}N_{B}}{P_{R}}}^{+\infty} \int_{\frac{\nu P_{R}N_{R}}{P_{A}N_{B}}}^{+\infty} f_{g_{AR}}(\mu) f_{g_{RB}}(\nu) T_{RB}(\nu) d\mu d\nu \\ &= \int_{k_{1}}^{+\infty} \int_{k_{2}\nu}^{+\infty} \frac{1}{2\sigma_{AR}^{2}} e^{-\frac{\mu}{2\sigma_{AR}^{2}}} \times \frac{1}{2\sigma_{RB}^{2}} e^{-\frac{\nu}{2\sigma_{RB}^{2}}} \times \log_{2}(1 + \frac{P_{R}\nu}{N_{B}}) d\mu d\nu \\ &\stackrel{(a)}{=} \int_{k_{1}}^{+\infty} e^{-\frac{k_{2}\nu}{2\sigma_{AR}^{2}}} \times \frac{1}{2\sigma_{RB}^{2}} e^{-\frac{\nu}{2\sigma_{RB}^{2}}} \times \log_{2}(1 + \frac{P_{R}\nu}{N_{B}}) d\nu \\ &\stackrel{(b)}{=} \frac{N_{B}}{2\sigma_{RB}^{2}} P_{R} \int_{\gamma_{\text{th}}}^{+\infty} e^{-k_{3}\nu'} \log_{2}(1 + \nu') d\nu' \\ &\stackrel{(c)}{=} \frac{N_{B}e^{k_{3}}}{2\log 2\sigma_{RB}^{2}P_{R}} \int_{1 + \gamma_{\text{th}}}^{+\infty} e^{-k_{3}\nu''} \log(\nu'') d\nu'' \\ &\stackrel{(d)}{=} \frac{N_{B}e^{k_{3}}}{2\log 2k_{3}\sigma_{RB}^{2}P_{R}} (e^{-k_{3}(1 + \gamma_{\text{th}})} - \text{Ei}(-k_{3}(1 + \gamma_{\text{th}}))) \\ &\stackrel{(e)}{=} \frac{\zeta_{2}}{\log 2(\zeta_{1} + \zeta_{2})} (e^{-\gamma_{\text{th}}(\zeta_{1} + \zeta_{2})} - e^{\zeta_{1} + \zeta_{2}} \text{Ei}(-(\zeta_{1} + \zeta_{2})(1 + \gamma_{\text{th}}))). \end{split} \tag{A.1}$$

In (A.1), (a) is derived by computing the integral with respect to  $\mu$ . (b) is derived by  $v' = \frac{P_R v}{N_B}$  and  $k_3 = \frac{N_B}{P_R} (\frac{k_2}{2\sigma_{AR}^2} + \frac{1}{2\sigma_{RB}^2}) = \frac{N_R}{2\sigma_{AR}^2 P_A} + \frac{N_B}{2\sigma_{RB}^2 P_R}$ , and the lower limit of integration becomes  $k_1 \times \frac{P_R}{N_B} = \gamma_{\rm th}$ . (c) is obtained by v'' = 1 + v' and the change of base formula for logarithms. (d) is derived by using the equation 2.751.2 in [42], i.e.,  $\int e^{ax} \log x dx = \frac{1}{a} [e^{ax} \log x - {\rm Ei}(ax)]$ . Defining  $\zeta_1 = \frac{N_R}{2\sigma_{AR}^2 P_A}$  and  $\zeta_2 = \frac{N_B}{2\sigma_{RB}^2 P_R}$ , (e) is obtained by  $k_3 = \zeta_1 + \zeta_2$ .

Denoting  $k_4 = \frac{\gamma_{\text{th}} N_R}{P_A}$ , the derivation of second integral in (34) is given as

$$\begin{split} &\int_{\frac{\gamma_{\text{th}}N_B}{P_R}}^{+\infty} \int_{\frac{\gamma_{P_R}N_R}{P_A}}^{\frac{\nu P_RN_R}{P_AN_B}} f_{g_{AR}}(\mu) f_{g_{RB}}(\nu) T_{AR}(\mu) d\mu d\nu \\ &= \int_{k_1}^{+\infty} \int_{k_4}^{k_2\nu} \frac{1}{2\sigma_{AR}^2} e^{-\frac{\mu}{2\sigma_{AR}^2}} \times \frac{1}{2\sigma_{RB}^2} e^{-\frac{\nu}{2\sigma_{RB}^2}} \times \log_2(1 + \frac{P_A\mu}{N_R}) d\mu d\nu \\ &\stackrel{(f)}{=} \frac{\zeta_1}{\log 2} \int_{k_1}^{+\infty} \int_{1+\gamma_{\text{th}}}^{1+\frac{P_R\nu}{N_B}} \frac{1}{2\sigma_{RB}^2} e^{-\frac{\nu}{2\sigma_{RB}^2}} \times e^{-\zeta_1\mu'} \log(\mu') d\mu' d\nu \\ &\stackrel{(g)}{=} \frac{1}{\log 2} \int_{k_1}^{+\infty} \frac{1}{2\sigma_{RB}^2} e^{-\frac{\nu}{2\sigma_{RB}^2}} [\text{Ei}(-\zeta_1(1 + \frac{P_R\nu}{N_B})) - e^{-\zeta_1(1 + \frac{P_R\nu}{N_B})} \times \\ &\log(1 + \frac{P_R\nu}{N_R}) + e^{-\zeta_1(1+\gamma_{\text{th}})} \log(1 + \gamma_{\text{th}}) - \text{Ei}(-\zeta_1(1 + \gamma_{\text{th}}))] d\nu. \end{split}$$

Transmission Probability and Power Optimization for Covert Communications in UAV-Aided THz Wireless Networks

(A.2)

In (A.2), (f) is obtained by  $\mu' = 1 + \frac{P_A \mu}{N_R}$ . (g) is derived by calculating the integral with respect to  $\mu'$  using the equation 2.751.2 in [42]. We can divide (A.2) into four independent integrals for calculation.

The derivation of first integral is

$$\int_{k_{1}}^{+\infty} \frac{1}{2\sigma_{RB}^{2}} e^{-\frac{v}{2\sigma_{RB}^{2}}} \operatorname{Ei}(-\zeta_{1}(1 + \frac{P_{R}v}{N_{B}})) dv$$

$$\stackrel{(h)}{=} e^{\zeta_{2}} \int_{1+\gamma_{\text{th}}}^{+\infty} \zeta_{2} e^{-\zeta_{2}v'} \operatorname{Ei}(-\zeta_{1}v') dv'$$
(A.3)

$$\stackrel{(i)}{=} e^{-\zeta_2 \gamma_{\rm th}} {\rm Ei}(-\zeta_1 (1+\gamma_{\rm th})) - e^{\zeta_2} {\rm Ei}(-(\zeta_1+\zeta_2)(1+\gamma_{\rm th})).$$

In (A.3), (h) is obtained by  $v' = 1 + \frac{P_R v}{N_B}$ . (i) is derived by  $\int ae^{-ax} \text{Ei}(-bx) dx = \text{Ei}(-(a+b)x) - e^{-ax} \text{Ei}(-bx)$ . The derivation of second integral is

$$\begin{split} &-\int_{k_{1}}^{+\infty}\frac{1}{2\sigma_{RB}^{2}}e^{-\frac{\nu}{2\sigma_{RB}^{2}}}e^{-\zeta_{1}(1+\frac{P_{RV}}{N_{B}})}\log(1+\frac{P_{RV}}{N_{B}})d\nu\\ \stackrel{(j)}{=}-e^{\zeta_{2}}\int_{1+\gamma_{\text{th}}}^{+\infty}\zeta_{2}e^{-(\zeta_{1}+\zeta_{2})\nu'}\log(\nu')d\nu'\\ \stackrel{(k)}{=}\frac{\zeta_{2}e^{\zeta_{2}}}{\zeta_{1}+\zeta_{2}}(e^{-(\zeta_{1}+\zeta_{2})(1+\gamma_{\text{th}})}\log(1+\gamma_{\text{th}})-\text{Ei}(-(\zeta_{1}+\zeta_{2})(1+\gamma_{\text{th}}))). \end{split} \tag{A.4}$$

In (A.4), (j) is obtained by  $v' = 1 + \frac{P_R v}{N_B}$ . (k) is derived by  $\int ae^{-bx} \log x dx = \frac{a}{b} (e^{-bx} \log x - \text{Ei}(-bx)).$ 

We can easily calculate the derivations of the third and fourth integrals since they are simple integrals of exponential functions. By summing these calculation results, (A.1), (A.3) and (A.4), we can get the derivation result of (34).

#### References

- Shunliang Zhang, Dali Zhu, and Yinlong Liu. Artificial Intelligence Empowered Physical Layer Security for 6G: State-of-the-art, Challenges, and Opportunities. Computer Networks, 242:110255, 2024.
- [2] Sidharth Thomas, Jaskirat Singh Virdi, Aydin Babakhani, and Ian P. Roberts. A Survey on Advancements in THz Technology for 6G: Systems, Circuits, Antennas, and Experiments. *IEEE Open Journal of the Communications Society*, 6:1998–2016, 2025.
- [3] Azade Fotouhi, Haoran Qiang, Ming Ding, Mahbub Hassan, Lorenzo Galati Giordano, Adrian Garcia-Rodriguez, and Jinhong Yuan. Survey on UAV Cellular Communications: Practical Aspects, Standardization Advancements, Regulation, and Security Challenges. IEEE Communications Surveys & Tutorials, 21(4):3417–3442, 2019.
- [4] Wagdy M. Othman, Abdelhamied A. Ateya, Mohamed E. Nasr, Ammar Muthanna, Mohammed ElAffendi, Andrey Koucheryavy, and Azhar A. Hamdi. Key Enabling Technologies for 6G: The Role of UAVs, Terahertz Communication, and Intelligent Reconfigurable Surfaces in Shaping the Future of Wireless Networks. *Journal of Sensor and Actuator Networks*, 14(2), 2025.
- [5] Boulat A. Bash, Dennis Goeckel, and Don Towsley. Limits of Reliable Communication with Low Probability of Detection on AWGN Channels. *IEEE Journal on Selected Areas in Communications*, 31(9):1921–1930, 2013.
- [6] Mohd Shariq, Ismail Taha Ahmed, Mehedi Masud, Aymen Dia Eddine Berini, and Norziana Jamil. Design of A Provable Secure Lightweight Privacy-Preserving Authentication Protocol for Autonomous Vehicles in IoT Systems. Computer Networks, 261:111155, 2025.

- [7] Jintao Xing, Tiejun Lv, Weicai Li, Wei Ni, and Abbas Jamalipour. Joint Optimization of Beamforming and Noise Injection for Covert Downlink Transmissions in Cell-Free Internet of Things Networks. *IEEE Internet of Things Journal*, 11(6):10525–10536, 2024.
- [8] Tamara V. Sobers, Boulat A. Bash, Saikat Guha, Don Towsley, and Dennis Goeckel. Covert Communication in the Presence of an Uninformed Jammer. *IEEE Transactions on Wireless Communications*, 16(9):6193–6206, 2017.
- [9] Tong-Xing Zheng, Ziteng Yang, Chao Wang, Zan Li, Jinhong Yuan, and Xiaohong Guan. Wireless Covert Communications Aided by Distributed Cooperative Jamming Over Slow Fading Channels. *IEEE Transactions on Wireless Communications*, 20(11):7026–7039, 2021.
- [10] Bin Yang, Tarik Taleb, Yuanyuan Fan, and Shikai Shen. Mode Selection and Cooperative Jamming for Covert Communication in D2D Underlaid UAV Networks. *IEEE Network*, 35(2):104–111, 2021.
- [11] Bin Yang, Tarik Taleb, Guilin Chen, and Shikai Shen. Covert Communication for Cellular and X2U-Enabled UAV Networks with Active and Passive Wardens. *IEEE Network*, 36(1):166–173, 2022.
- [12] Jingsen Jiao, Ranran Sun, Yizhi Cao, Qifeng Miao, Yanchun Zuo, and Weidong Yang. Study on Covert Rate in the D2D Networks with Multiple Non-Colluding Wardens. Computer Networks, 250:110532, 2024
- [13] Nguyen Quang Hieu, Dinh Thai Hoang, Dusit Niyato, Diep N. Nguyen, Dong In Kim, and Abbas Jamalipour. Joint Power Allocation and Rate Control for Rate Splitting Multiple Access Networks With Covert Communications. *IEEE Transactions on Communications*, 71(4):2274–2287, 2023.
- [14] Khurram Shahzad, Xiangyun Zhou, Shihao Yan, Jinsong Hu, Feng Shu, and Jun Li. Achieving Covert Wireless Communications Using a Full-Duplex Receiver. *IEEE Transactions on Wireless Communica*tions, 17(12):8517–8530, 2018.
- [15] Yihuai Yang, Bin Yang, Shikai Shen, Yumei She, and Tarik Taleb. Covert Rate Study for Full-Duplex D2D Communications Underlaid Cellular Networks. *IEEE Internet of Things Journal*, 10(17):15223– 15237, 2023
- [16] Rongrong He, Guoxin Li, Haichao Wang, Yutao Jiao, and Jihao Cai. Adaptive Power Control for Cooperative Covert Communication With Partial Channel State Information. *IEEE Wireless Communications Letters*, 11(7):1428–1432, 2022.
- [17] Ran Zhang, Xinying Chen, Mingqian Liu, Nan Zhao, Xianbin Wang, and Arumugam Nallanathan. UAV Relay Assisted Cooperative Jamming for Covert Communications Over Rician Fading. *IEEE Transactions on Vehicular Technology*, 71(7):7936–7941, 2022.
- [18] Ranran Sun, Bin Yang, Yulong Shen, Xiaohong Jiang, and Tarik Taleb. Covertness and Secrecy Study in Untrusted Relay-Assisted D2D Networks. *IEEE Internet of Things Journal*, 10(1):17–30, 2023.
- [19] Ranran Sun, Bin Yang, Siqi Ma, Yulong Shen, and Xiaohong Jiang. Covert Rate Maximization in Wireless Full-Duplex Relaying Systems With Power Control. *IEEE Transactions on Communications*, 69(9):6198–6212, 2021.
- [20] Bohang Wang, Yunyang Zhang, Rui Xu, Siqi Jiang, Aijun Liu, Guoru Ding, and Xiaohu Liang. Relay-Assisted Finite Blocklength Covert Communications for Internet of Things. *IEEE Internet of Things Journal*, 11(24):39984–39993, 2024.
- [21] Xian Yu, Shihao Yan, Jinsong Hu, Paul Haskell-Dowland, Yubing Han, and Derrick Wing Kwan Ng. On Relaying Strategies in Multi-Hop Covert Wireless Communications. In ICC 2022 - IEEE International Conference on Communications, pages 666–672, 2022.
- [22] Chan Gao, Bin Yang, Dong Zheng, Xiaohong Jiang, and Tarik Taleb. Cooperative Jamming and Relay Selection for Covert Communications in Wireless Relay Systems. *IEEE Transactions on Communica*tions, 72(2):1020–1032, 2024.
- [23] Yinjie Su, Hongjian Sun, Zhenkai Zhang, Zhuxian Lian, Zhibin Xie, and Yajun Wang. Covert Communication With Relay Selection. *IEEE Wireless Communications Letters*, 10(2):421–425, 2021.
- [24] Lu Lv, Qingqing Wu, Zan Li, Zhiguo Ding, Naofal Al-Dhahir, and Jian Chen. Covert Communication in Intelligent Reflecting Surface-Assisted NOMA Systems: Design, Analysis, and Optimization. IEEE

Transmission Probability and Power Optimization for Covert Communications in UAV-Aided THz Wireless Networks

- Transactions on Wireless Communications, 21(3):1735–1750, 2022.
- [25] Chao Wang, Zan Li, Tong-Xing Zheng, Derrick Wing Kwan Ng, and Naofal Al-Dhahir. Intelligent Reflecting Surface-Aided Full-Duplex Covert Communications: Information Freshness Optimization. *IEEE Transactions on Wireless Communications*, 22(5):3246–3263, 2023.
- [26] Chan Gao, Linying Tian, Qiuxia Zhao, Dong Zheng, and Xiaohong Jiang. Covert and Secure Communication in Untrusted UAV-Assisted Wireless Systems. *IEEE Internet of Things Journal*, 2025.
- [27] Zhihong Liu, Jiajia Liu, Yong Zeng, and Jianfeng Ma. Covert Wireless Communication in IoT Network: From AWGN Channel to THz Band. IEEE Internet of Things Journal, 7(4):3378–3388, 2020.
- [28] Weijun Gao, Yi Chen, Chong Han, and Zhi Chen. Distance-Adaptive Absorption Peak Modulation (DA-APM) for Terahertz Covert Communications. *IEEE Transactions on Wireless Communications*, 20(3):2064–2077, 2021.
- [29] Milad Tatar Mamaghani and Yi Hong. Aerial Intelligent Reflecting Surface-Enabled Terahertz Covert Communications in Beyond-5G Internet of Things. *IEEE Internet of Things Journal*, 9(19):19012– 19033, 2022.
- [30] Xinzhe Pi, Bin Yang, and Xiaohong Jiang. Covert Terahertz Communication for UAV-Aided Wireless Relay Systems. In 2023 International Conference on Networking and Network Applications (NaNA), pages 127–132, 2023.
- [31] Yun Dong, Liyuan Zhang, Zijian Lin, Yuan Yin, and Zhaoli Chen. Multiuser Covert Terahertz Communication With Outdated CSI and Data Exception. *Transactions on Emerging Telecommunications Technologies*, 36(7):e70184, 2025.
- [32] Ruiqian Ma, Weiwei Yang, Liwei Tao, Xingbo Lu, Zhongwu Xiang, and Jue Liu. Covert Communications With Randomly Distributed Wardens in the Finite Blocklength Regime. *IEEE Transactions on Vehicular Technology*, 71(1):533–544, 2022.
- [33] Demos Serghiou, Mohsen Khalily, Tim W. C. Brown, and Rahim Tafazolli. Terahertz Channel Propagation Phenomena, Measurement Techniques and Modeling for 6G Wireless Communication Applications: A Survey, Open Challenges and Future Research Directions. IEEE Communications Surveys & Tutorials, 24(4):1957–1996, 2022.
- [34] Alexandros-Apostolos A. Boulogeorgos, Evangelos N. Papasotiriou, and Angeliki Alexiou. A Distance and Bandwidth Dependent Adaptive Modulation Scheme for THz Communications. In 2018 IEEE 19th International Workshop on Signal Processing Advances in Wireless Communications (SPAWC), pages 1–5, 2018.
- [35] Boulat.A Bash. Fundamental Limits of Covert Communication. PhD thesis, University of Massachusetts Amherst, 2015. Available at https://scholarworks.umass.edu/dissertations\_2/283/.
- [36] Moslem Forouzesh, Farid Samsami Khodadad, Paeiz Azmi, Ali Kuhestani, and Hossein Ahmadi. Simultaneous Secure and Covert Transmissions Against Two Attacks Under Practical Assumptions. IEEE Internet of Things Journal, 10(12):10160–10171, 2023.
- [37] Tingzhen Xu, Linlin Sun, Shihao Yan, Jinsong Hu, and Feng Shu. Pilot-Based Channel Estimation Design in Covert Wireless Communication, August 2019. arXiv preprint.
- [38] Yuda Lin, Liang Jin, Kaizhi Huang, and You Zhou. Multi-Antenna Joint Covert Communication with A Public Communication Link over Wireless Fading Channel. *IET Communications*, 15(5):695–707, 2021.
- [39] Nanchi Su, Fan Liu, and Christos Masouros. Sensing-Assisted Eavesdropper Estimation: An ISAC Breakthrough in Physical Layer Security. *IEEE Transactions on Wireless Communications*, 23(4):3162– 3174, 2024.
- [40] Ning Wang, Long Jiao, Pu Wang, Weiwei Li, and Kai Zeng. Exploiting Beam Features for Spoofing Attack Detection in mmWave 60-GHz IEEE 802.11ad Networks. IEEE Transactions on Wireless Communications, 20(5):3321–3335, 2021.
- [41] P.E. Pace. Detecting and Classifying Low Probability of Intercept Radar, Second Edition. Artech House Radar Library. Artech House, 2009
- [42] I. S. Gradshteyn and I. M. Ryzhik. Table of Integrals, Series, and Products (Eighth Edition). Academic Press, 2014.



Xinzhe Pi received his B.S. and M.S. degrees in 2014 and 2017 respectively, all from Hefei University of Technology, China. He received his Ph.D. degree in systems information science from Future University Hakodate, Japan in 2025. He is currently an assistant lecturer in the School of Computer and Information Engineering, Chuzhou University, China. His research interests include wireless communication, covert communication, and artificial intelligence.



Bin Yang received his Ph.D. degree in systems information science from Future University Hakodate, Japan in 2015. He was a research fellow with the School of Electrical Engineering, Aalto University, Finland, from Nov. 2019 to Nov. 2021. He is currently a professor with the School of Computer and Information Engineering, Chuzhou University, China. His research interests include unmanned aerial vehicle networks, cyber security, mobile edge computing and Internet of Things.



Yulong Shen received the B.S. and M.S. degrees in computer science and the Ph.D. degree in cryptography from Xidian University, Xi'an, China, in 2002, 2005, and 2008, respectively. He is currently a Professor with the School of Computer Science and Technology, Xidian University. He is also an Associate Director of Shaanxi Key Laboratory of Network and System Security and a member of the State Key Laboratory of Integrated Services Networks, Xidian University. His research interests include wireless network security and cloud computing security. He has also served on the technical program committees for several international conferences, including ICEBE, INCoS, CIS, and SOWN



Xiaohong Jiang received his B.S., M.S. and Ph.D degrees in 1989, 1992, and 1999 respectively, all from Xidian University, China. He is currently a full professor of Future University Hakodate, Japan. Before joining Future University, Dr. Jiang was an Associate professor, Tohoku University, from Feb. 2005 to Mar. 2010. Dr. Jiang's research interests include computer communications networks, mainly wireless networks and optical networks, network security, routers/switches design, etc. He has published over 300 technical papers at premium international journals and conferences, which include over 70 papers published in top IEEE journals and top IEEE conferences, like IEEE/ACM Transactions on Networking, IEEE Journal of Selected Areas on Communications, IEEE Transactions on Parallel and Distributed Systems, IEEE INFOCOM.

Transmission Probability and Power Optimization for Covert Communications in UAV-Aided THz Wireless Networks



Tarik Taleb received the B.E. degree Information Engineering with distinction and the M.Sc. and Ph.D. degrees in Information Sciences from Tohoku University, Sendai, Japan, in 2001, 2003, and 2005, respectively. He is currently a Full Professor with the Faculty of Electrical Engineering and Information Technology, Ruhr University Bochum. He is the founder and director of the MOSAIC Lab (www.mosaic-lab.org). Between Oct. 2014 and Dec. 2021, he was a Professor at the School of Electrical Engineering, Aalto University, Finland. Prior to that, he was working as Senior Researcher and 3GPP Standards Expert at NEC Europe Ltd, Heidelberg, Germany. Before joining NEC and till Mar. 2009, he worked as assistant professor at the Graduate School of Information Sciences, Tohoku University, Japan, in a lab fully funded by KDDI, the second largest mobile operator in Japan. From Oct.2005 till Mar.2006, he worked as research fellow at the Intelligent Cosmos Research Institute, Sendai, Japan. His research interests lie in the field of telco cloud, network softwarization & network slicing, AI-based software defined security, immersive communications, mobile multimedia streaming, and next generation mobile networking. He has been also directly engaged in the development and standardization of the Evolved Packet System as a member of 3GPP's System Architecture working group. He served as the general chair of the 2019 edition of the IEEE Wireless Communications and Networking Conference (WCNC'19) held in Marrakech, Morocco. He was the guest editor in chief of the IEEE JSAC Series on Network Softwarization & Enablers. He was on the editorial board of the IEEE Transactions on Wireless Communications, IEEE Wireless Communications Magazine, IEEE Journal on Internet of Things, IEEE Transactions on Vehicular Technology, IEEE Communications Surveys & Tutorials, and a number of Wiley journals. Till Dec. 2016, he served as chair of the Wireless Communications Technical Committee.

# **Declaration**of Interest Statement

The authors declare that they have no known competing financial interests or personal relationships that could have appeared to influence the work reported in this paper.